
# BRNO UNIVERSITY OF TECHNOLOGY
VYSOKÉ UČENÍ TECHNICKÉ V BRNĚ

## FACULTY OF MECHANICAL ENGINEERING
FAKULTA STROJNÍHO INŽENÝRSTVÍ

## INSTITUTE OF MATHEMATICS
ÚSTAV MATEMATIKY


# LUBRICANT GAP SHAPE OPTIMIZATION OF THE HYDRODYNAMIC THRUST BEARING
OPTIMALIZACE TVARU MAZACÍ MEZERY HYDRODYNAMICKÉHO LOŽISKA

**MASTER'S THESIS**
DIPLOMOVÁ PRÁCE


**AUTHOR** — **Ikechi Ochulo**
AUTOR PRÁCE

**SUPERVISOR** — **doc. Ing. Pavel Novotný, Ph.D.**
VEDOUCÍ PRÁCE


**BRNO 2021**

BRNO UNIVERSITY OF TECHNOLOGY
FACULTY OF MECHANICAL ENGINEERING

# Assignment Master's Thesis

| | |
|---|---|
| Institut: | Institute of Mathematics |
| Student: | **Ikechi Ochulo** |
| Degree programm: | Applied Sciences in Engineering |
| Branch: | Mathematical Engineering |
| Supervisor: | **doc. Ing. Pavel Novotný, Ph.D.** |
| Academic year: | 2020/21 |

As provided for by the Act No. 111/98 Coll. on higher education institutions and the BUT Study and Examination Regulations, the director of the Institute hereby assigns the following topic of Master's Thesis:

## Lubricant Gap Shape Optimization of the Hydrodynamic Thrust Bearing

**Brief Description:**

Hydrodynamic bearings are designed with maximum mechanical efficiency in mind. Elementary shapes of bearings working surfaces are often assumed when optimizing the bearing performance. The analytical description of elementary shapes thus considerably limits the shape of the work surface. The work deals with the optimization of the working surface of completely general shape. The work assumes the creation of a program or script in a programming language (e.g. Matlab, C ++, Python or Fortran) and application to thrust bearings of turbochargers. It includes a comparison of the integral parameters of the optimal thrust bearing with the existing series–used bearing.

**Master's Thesis goals:**

Review of suitable optimization methods for solving the problem.
Program for optimizing the bearing working surface of general shape.
Application of the optimization procedure in the design of the working surface of the thrust bearing of a turbocharger.

**Recommended bibliography:**

LUKE, S. Essentials of metaheuristics. 2. ed., 2013. ISBN 9781300549628.

NGUYEN-SCHÄFER, H. Rotordynamics of Automotive Turbochargers. Second Edition. Ludwigsburg, Germany: Springer, 2015. ISBN 978-3-319-17643-7.

STACHOWIAK, G. W. a A. W. BATCHELOR. Engineering Tribology. 3. vyd. Boston: Elsevier Butterworth-Heinemann, 2005. ISBN 0-7506-7836-4.

Deadline for submission Master's Thesis is given by the Schedule of the Academic year 2020/21

In Brno,

L. S.

| | |
|---|---|
| prof. RNDr. Josef Šlapal, CSc.<br>Director of the Institute | doc. Ing. Jaroslav Katolický, Ph.D.<br>FME dean |

**Abstrakt**

Abstrakt česky...

**Abstract**

The objective of this Master's thesis is to find an optimal lubricating gap profile for a turbocharger. The aim is to minimize friction, maintain load capacity, and not increase lubricant flow rate. This multiobjective optimization is performed by using genetic algorithm(GA) in MATLAB. Minimizing friction force reduces the friction power losses of the turbocharger. The solution of the Reynolds equation is computed numerically using MATLAB. The minimum lubricating gap thickness for an initial problem is found. A spline function is used to generate a general profile of the lubricating gap. This profile is then optimized using GA in MATLAB.

**klíčová slova**

...

**keywords**

shape optimization, thrust bearing, genetic algorithm, MATLAB, Reynolds Equation, splines.

Ochulo Ikechi: LUBRICANT GAP SHAPE OPTIMIZATION OF THE HYDRODYNAMIC THRUST BEARING, Brno University of Technology, Faculty of Mechanical Engineering, 2021. 56 pp. Supervisor: Assoc. prof. MSc. Ing. Pavel Novotný, Ph.D.

I declare that I have worked on this thesis independently under the supervision of doc. Ing. Pavel Novotný, Ph.D. and using the sources listed in the bibliography.

Ikechi Ochulo

I want to thank my family, for their incessant good wishes and prayers. I want to thank my supervisor, for shining a light in the dark. Special thanks to the InterMaths Consortium for this opportunity and especially Nwachukwu Anthony; you're a gift.

Ikechi Ochulo

# Table of Contents

# 1 Introduction

## 1.1 The Turbocharger

Basically, a turbocharger is a rotor that features a turbine on one side and a compressor on the other side.

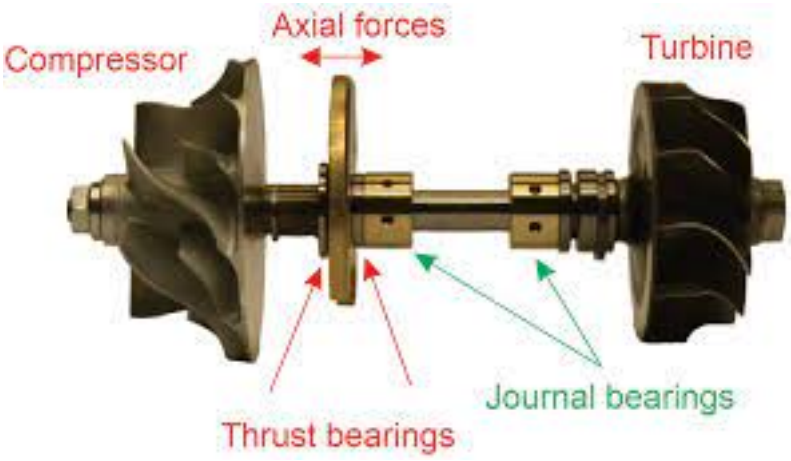


Figure 1: Simple diagram of the Turbocharger
[28]

Turbochargers have improved the efficiency of combustion engines while reducing their size and maintaining the power. In recent times, most diesel engines are turbocharged; more gasoline engines are also being equipped with the turbocharger.

In passenger vehicles, the turbocharger scavenges from the exhaust gas flow. It delivers it to the compressor. The compressor compresses the surrounding air and feeds it to the engine. In some vehicles, the exhaust gas is used to drive some turbochargers and used to supply air to the combustion chamber for scavenging and supercharging.

The fluid film bearing system of a turbocharger commonly comprises the three regimes of lubrication: boundary, mixed and hydrodynamic.[27]

The mixed and boundary regimes of lubrication do not provide an optimal operating environment for the turbocharger. In these regimes, there is the risk of high wear of the component parts of the turbocharger. To prevent operating in these regimes , the oil film thickness should be larger than the limit oil film thickness of 3 micrometers (3e-6 m). [20]

## 1.2 The Bearing

A bearing is a machine part that bears (supports) one or more of the moving parts of a mechanical assembly. Its principal function is to reduce mechanical friction between the moving parts. By reducing friction, it improves the efficiency of running, reduces abrasion and wear due to friction and improves the life of the machinery.

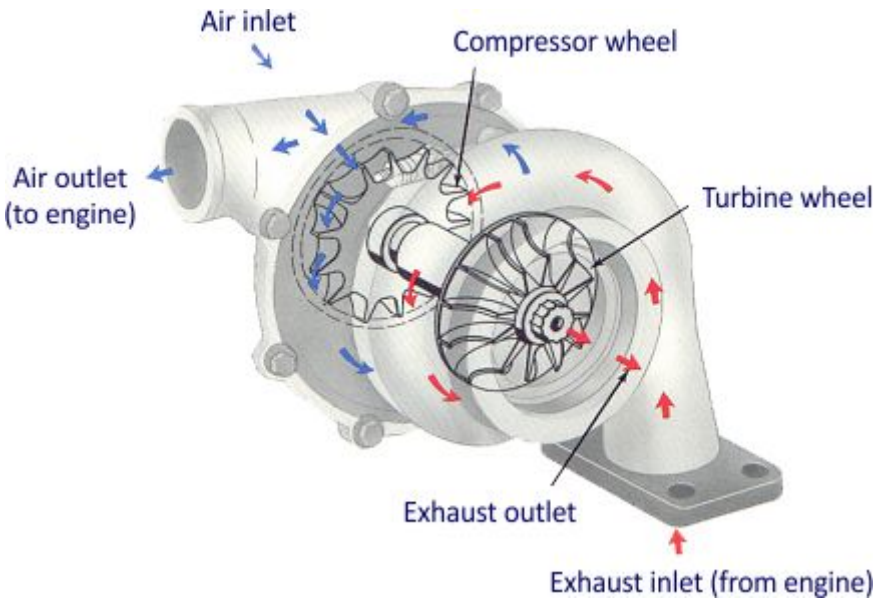


Figure 2: Turbocharger

To reduce the effects of friction among the moving parts of mechanical assemblies, the surfaces of these parts are lubricated. It is expected that the lubricating fluid be viscous enough, and maintain this property under high temperature; the fluid should be able to carry the heat generated by these moving parts away from the surfaces, hence cooling these surfaces.

## 1.3 The Hydrodynamic Bearing

When the surfaces of the two moving parts glide over each other with sufficient velocity for a load-carrying lubricating film to be generated and these surfaces are inclined at an angle to each other, hydrodynamic lubrication occurs.

Pressure in the hydrodynamic film is generated due to relative motion of the surfaces separated by the layer of viscous fluid. Low speed during machine start up and shutdown makes it difficult to generate adequate pressure allowing for full film lubrication[31].

A hydrodynamic bearing supports a shaft in hydrodynamic lubrication.

The converging (bearing) geometry of a journal bearing is formed when the journal center location is non-concentric in the bearing. The journal rotation drags oil into the wedge and generates pressure which then separates the sliding pair[30].

In our problem, we consider the movement of two parts of a mechanical assembly: the thrust rings and the shaft. The thrust bearing supports the axial motion of the shaft. When the conditions for hydrodynamic lubrication, as mentioned above, are satisfied, hydrodynamic lubrication occurs.

Schematically, this setup could be represented as an inclined plane-slider carrying a

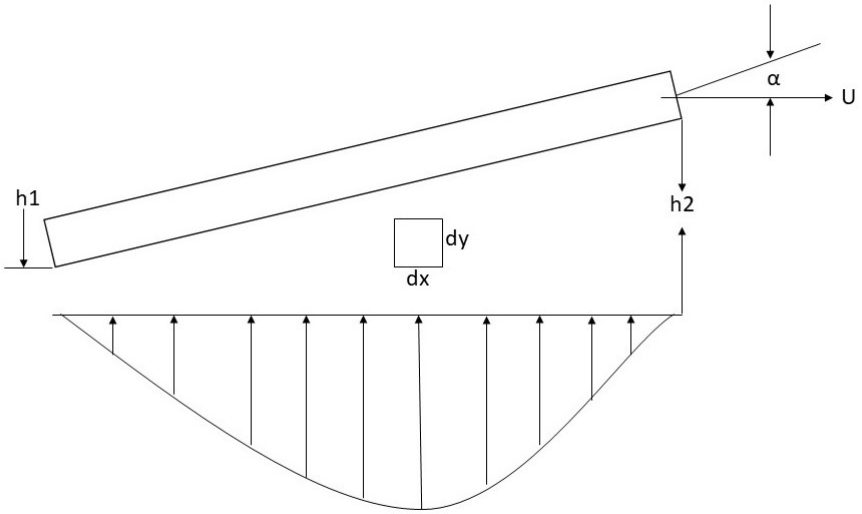


Figure 3: Schematic of Hydrodynamic Bearing
[20]

load F, with a horizontal velocity U, relative to a stationary horizontal plane surface. This plane-slider has an angle of inclination $\alpha$ relative to the horizontal plane.

At full hydrodynamic lubrication, a full separation between the plane-slider and the horizontal plane surface is obtained. The inclined slider forms a converging viscous wedge of lubricant; the magnitudes of $h_1$ and $h_2$ are very small. The clearance is very much enlarged.

The wedge that is formed by the lubricating fluid takes the shape of the clearance between the two components being lubricated. The shape of this clearance is called the lubricating gap [20].

### 1.3.1 The Thrust Bearing

The minimum film thickness of a bearing setup is the minimum gap size between the rotating shaft and the housing, which can support shaft rotation and reduce contact between surface asperities. It depends on factors such as surface roughness and type of loading.

When a journal does not return to its established equilibrium position or attitude, hydrodynamic instability is said to occur. In lightly loaded, high-speed bearings, shocks or vibrations produce an instability which is known to reduce the whirl speed of the assembly by as much as half the original speed. This phenomenon is called half-speed whirl. The extent of shaft whirl ranges from unnoticed to a violent reaction that destroys the bearing.

The thrust bearing design is complicated. Complete analysis requires consideration of heat generation, oil flow, bearing material, load capacity, and stiffness. There are different kinds of thrust bearings; the two briefly described in this work are the tapered-land,

tilting pad. In a tapered-land thrust bearing, design variables include the slope, width, and length of the lands. The tapered-land bearing has a fixed geometry.

Fixed geometry bearings, such as tapered land, are designed for a specific set of operating conditions. Deviations from these conditions result in less than optimum bearing performance. Unlike fixed geometry bearings, the tilting-pad thrust bearings have the ability to self-adjust the slope or tilt to accommodate varying operating conditions. Equalizing tilting pad thrust bearings permits even thrust-load distribution over pads. This equalization handles misalignment and deflections in the housing and seating [29].

Tilting pad thrust bearings comprise of individual pads. The number of pads could be 10, sometimes more. This inevitably results in some difference in pad height due to assembly and manufacturing tolerances of the complete bearing system. Flexible rotors operating at high rotational speeds are often supported in tilting pad journal bearings due to their stabilizing effect compared to other bearing types with fixed geometry [30].

Like in other types of hydrodynamic bearings, the operational range of large tilting pad thrust bearings has three kinds of limit: film thickness, mechanical, and temperature limits [31].

For this thesis problem, the limit under consideration is the film thickness limit.

## 1.4 Problem Definition

The history of design is almost as old as the history of homo sapiens. It has always been the goal of engineering to improve design to satisfy the human need in the best way possible, within available means.

The classical approach to optimization of the thrust bearing was:
1 Describing the bearing analytically by parameters
2 Optimizing these parameters by any optimization method
In recent times and for this work, the new approach to optimization:

1. Describing the working profile of the bearing a general function

2. Optimizing parameters by any optimization method.

The clearance, slenderness ratio, viscosity play important roles in estimating the performance of a journal bearing. Therefore, in most optimization procedures, they top the list of parameters to be optimized.

The lubrication gap in a hydrodynamic thrust bearing exerts great influence of the on the bearing properties. It has been shown from experiments that a close-to-optimum oil gap profile for assumed load/speed conditions, the results show substantial increase in the minimum oil film thickness and lower temperature in the bearing. This improvement of properties is thought to be because of the optimized oil gap profile in the bearing [7].

Design optimization is, in layman terms, the procedure of finding and/or selecting the best way possible, within available means. The process of finding the best design possible can be mathematically expressed in the objective function; the available means form the constraints of the objective function. In our case, we consider the design of the lubrication gap of the hydrodynamic thrust bearing of the automotive turbocharger. The optimization of its design can be classified under shape optimization.

Shape optimization is a part of the field of optimal control theory. A typical problem entails finding an optimal shape that minimizes a certain cost function while satisfying given constraints.

The main goal of shape optimization is to provide a common and systematic framework to optimize structures by various possible models. There has been a rise in this field of study due to the rise in cost of materials and the need to optimize mechanical parts not only in applications but also from the initial stages of design.

## 1.5 Problem Statement

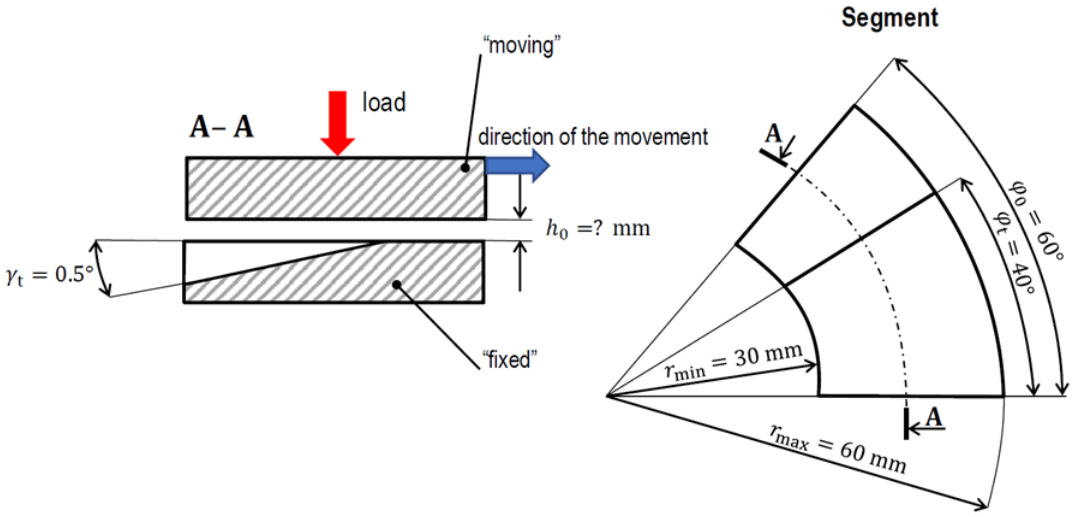


Figure 4: Initial Problem

**The initial geometry for the given operating condition:**

Load segment $F_{ax} = 100N$

Rotor speed, n = 45000 rpm

Lubricant dynamic viscosity, $\mu = 0.01$ Pa.s

**The criteria under which the problem is to be solved:**

i Minimize friction force.

ii Maintain load capacity.

iii Do not increase lubrication flow rate.

iv Do not decrease minimum gap thickness.

**For the scope of this work:**

i The problem will be considered in two dimensions.

ii Optimization will be done using genetic algorithms.

## 1.6 Goal of Thesis

The process of finding an optimal design (shape) for a given problem involves sorting and testing of all elements of the set of admissible shapes and keeping the most optimal of them. This problem can be solved by use of various algorithms that would compute the optimal solution.

For this problem, we would use the genetic algorithm. Genetic algorithms are stochastic methods that can be used to solve approximately in optimization. It attempts to replicate the mechanics of natural selection and genetics. A randomly selected parent population (elements from the set of admissible shapes) reproduces and mutates to form offspring (new shapes) under the condition that only the fittest survive.

This algorithm randomly tests all possible solutions: keeping the optimal shapes and discarding the least optimal ones. With the aid of genetic algorithms, I hope to find an optimal lubrication gap, $h_{opt}$, and the consequent lubricating gap profile, for the initial geometry under the given operating conditions.

# 2 Literature Review

## 2.1 Introductory Notes on Optimization

The role of shapes of materials has been assumed for the most of technological advancement. It was generally assumed that smooth surfaces should result in better tribological performance of engineering instruments and equipment. This assumption was extended to the general objects in our surrounding. The thought that fostered this assumption was that to eliminate friction, the surfaces in contact should be smoothened, given a better finish [11].

But this is not true. The cutting of groves (or dimples) in the golf ball made it possible for the club to get a better 'grip' of the ball; this was consistent with the prevailing thought and expectations. What was unexpected was the fact that these groves made the flight of the ball through air (a fluid) better; the ball could move more smoothly, and it also moved farther than the smooth ball.

Apparently, this was already practiced by nature. The microstructures on the skin of the shark helped reduce drag in its movement through water (a fluid) [10].

## 2.2 Optimization Terms

Before formulating the optimum design problems for high-speed, journal bearings, the terms and definitions used in optimum design would be introduced:

- Design variable: the main factor that determines bearing design. Radial clearance, bearing length, bearing radius and viscosity come under the scope of design variables.

- State variable: physical quantities that vary under operating conditions such as the load, rotational speed, eccentricity ratio quantity of lubricant supply, etc.

- Constraint: a condition that must be satisfied in the optimum design. It might include restrictions relatable to film thickness, film temperature or pressure, etc.

- Objective function: the quantity, function, to be minimized or maximized under the constraints. This includes fluid temperature rise, quantity of lubricant supplied, manufacturing cost, etc.

- Optimum design problem: the problem of finding the optimum variables that optimize the objective function under the prescribed constraints [14].

## 2.3 Optimization in Thrust Bearings

The principal performance indices of a thrust bearing are its load carrying capacity and its friction coefficient. Optimizing thrust bearing performance would mean the maximization

of load carrying capacity; this would lead to larger film thickness for a given load and by implication less bearing wear. Increasing the film thickness would also better the bearing performance in transient loads/impact loads.

Optimization might also mean reduction in bearing dimensions for a given value of minimum film thickness. This results in reduced friction power losses.

Furthermore, minimization of the friction coefficient will contribute to reduced power losses. [27]

## 2.4 Seminal Works

The idea of modification of the shapes (and texture of surfaces) of tribological parts of mechanical devices has been established in nature as was hinted in the introduction. However, the application of this knowledge is quite recent.

Larry Fogel's dissertation was undoubtedly the first such thesis, if not the first major work, in the field of evolutionary computation. Lawrence Fogel, 1964, On the Organization of Intellect, Ph.D. thesis, University of California, Los Angeles [19].

The Genetic Algorithm was invented by John Holland at the University of Michigan in 1975. His book Adaptation in Natural and Artificial Systems University of Michigan Press is one of the more famous books in the field.

The idea of using Genetic Algorithms in Engineering design was first introduced by The Plymouth Engineering Design Center (PEDC) in 1991. The center was established to carry out fundamental research into the application of Genetic Algorithm and adaptative search techniques to engineering design. It has as one of its missions, the making of GA more accessible to practicing engineers across a wide range of disciplines. This goal has since made the center to string along different branches of engineering and has kept its research and works to remain the domain of applicability. The goal has been to make the algorithm accessible in a useful and understandable form to designers engaged in the many branches of engineering. It was envisaged that GA oriented design process can be developed with which the engineer will be able to interact to reduce design time whilst also significantly improving both performance and the economics of the design solution.

The Plymouth Engineering Design Center PEDC was established in 1991 PEDC has been considering how best the GA may be linked to knowledge-based systems and other adaptative search processes[12]. They also investigated ways to integrate GA into existing design practices.

Much of the early work into evolutionary design was done by Rechenberg, Ingo at Technical University of Berlin in 1965.

## 2.5 Progress made by seminal works

"*One of the ways to reduce the friction losses in a turbocharger thrust bearing is by application of surface texture features. Recent research has been carried out to investigate the effect of periodic irregularities of various shapes (rectangular, trapezoidal, cylindrical or spherical), imprinted on part of the stator of fixed inclination thrust bearings on bearing performance. The reported numerical and experimental studies, demonstrated potential for improving bearing performance. As current technology has enabled the accurate manufacturing of such micro-scale patterns, contemporary research on the performance of textured bearings is growing more intense, with the optimization of texture geometry and placement being attempted by several researchers.*[27]"

Most of the recorded progress in this field has been in the texture of the surface of the lubricated mechanical parts. In this aspect, much progress has been made. Many research groups have deliberated, by theory and experimentation, the effect of various shape contours of textures on tribological performance. They confirmed that different texture shapes affect the tribological performance of the lubricating system.

In their work, Charitopoulos et al [27], experimented the optimization of tapered-land bearing. The geometric parameters used for the optimization of the tapered-land bearing were:

- (a) the extent of the tapered part of the bearing as percentage of the length, and
- (b) the maximum taper depth in microns.

Most of the work in thrust bearing optimization, have considered optimizing the tapered-land bearing. Its fixed geometry has made it attractive for analysis.

## 2.6 Limitations of the seminal works

Modification of the shape of mechanical equipment and parts has been 'restricted' to aerodynamics. The shape of the body in motion has been necessary in the improvement of the performance of cars, bicycles, airplanes, and other mechanical devices. This has been proven to reduce the drag of the vehicle, reduce the fuel consumption, and improve the general efficiency of the vehicle.

However, this idea of shape modification and optimization has not been exhaustively applied to lubricated parts of these vehicles. This means that the idea of shape optimization has not seen extensive application in the tribology. The limited application of the knowledge of shape optimization to tribology means that a lot more progress can be made in reducing friction, increasing load bearing capacity, and improving the efficiency of mechanical systems.

The consideration of simple profiles presents an easier problem. But, it has limited the scope of what is known of the working conditions of the tilted-pad bearings with variable geometry.

## 2.7 How does my work fill the gap?

Minimizing friction losses is the generally pursued to increase turbocharger efficiency. By minimizing the friction losses, the mechanical efficiency is improved.

The mechanical efficiency of the turbocharger is an important parameter in the general efficiency of the turbocharger. This means that an improvement of the mechanical efficiency of the turbocharger will influence the general efficiency of the turbocharger.

The best profile of the lubrication gap of the turbocharger would result in the better mechanical effects in the system; it would minimize friction in the system and thus improve the mechanical effects and efficiency of the system.

The byproducts of the optimal lubrication gap profile could include:

i Reduction the quantity of material used.

ii These should result in reducing emission of the turbocharger and carbon footprint of lubrication system of the turbocharger.

iii A method for optimizing a general profile described by any of the shapes taken by a tilting-pad thrust bearing.

# 3 Materials and Methods

## 3.1 Assumptions of Classical hydrodynamic lubrication theory

1. The flow is laminar because the Reynolds number, Re, is low.

2. The fluid lubricant is continuous, Newtonian, and incompressible.

3. The fluid adheres to the solid surface at the boundary and there is no fluid slip at the boundary; that is, the velocity of fluid at the solid boundary is equal to that of the solid.

4. The velocity component, n, across the thin film (in the y direction) is negligible in comparison to the other two velocity components, u and w, in the x and z directions as can be seen in Figure9.

5. Velocity gradients along the fluid film, in the x and z directions, are small and negligible relative to the velocity gradients across the film because the fluid film is thin, i.e., $du = dy >> du = dx$ and $dw = dy >> dw = dz$..

6. The effect of the curvature in a journal bearing can be ignored. The film thickness, h, is very small in comparison to the radius of curvature, R, so the effect of the curvature on the flow and pressure distribution is relatively small and can be disregarded.

7. The pressure, $p$, across the film (in the $y$ direction) is constant. In fact, pressure variations in the y direction are very small and their effect is negligible in the equations of motion.

8. The force of gravity on the fluid is negligible in comparison to the viscous forces.

9. Effects of fluid inertia are negligible in comparison to the viscous forces. In fluid dynamics, this assumption is usually justified for low-Reynolds-number flow.

10. The fluid viscosity, $\eta$, is constant. This is for simplification of the analysis.

This last assumption can be applied in practice because it has already been verified that reasonably accurate results can be obtained for regular hydrodynamic bearings by considering an equivalent viscosity. [1]

For a proper analysis of the problem, and optimization of the lubrication gap profile of the thrust bearing, the tools of analysis to be used include:

- Reynold's equation
- Newton's Method
- Shapes and Splines

- Genetic algorithm
- MATLAB

## 3.2 Reynold's Lubrication Equation

The Reynolds lubrication equation is used to compute the flow dynamics and included bearing forces in the oil film bearings. It works with insignificantly small convection terms at low Reynolds number. This is because the oil flows in oil film bearings of automotive turbochargers are usually laminar having Reynolds number ranging from 100 to 200 [20].

To analyze the problem, the oil film can be simplified as a fluid wedge that is surrounded by a bearing and journal moving with velocities $U_1$ and $U_2$ respectively. The ambient pressure of oil at the inlet and outlet is defined as $p_0$. The movement of the journal bearing causes lubricating oil to be drawn into the system from the inlet at ambient pressure and flows with a velocity u(x,y) through the wedge. The oil film is squeezed with a velocity u; hence the oil film pressure p(x,z) increases in the directions x and z from the inlet to the middle of the fluid wedge. The oil pressure in the wedge remains unchanged, in the y-direction, since the oil film thickness is very small. Hence, the Reynolds number of the oil flow is very low, the flow is laminar with a parabolic velocity profile[26].

The velocity of the journal $U_2$ comprises of two components: $U_j$ parallel to the journal surface and $v_j$ perpendicular to the moving direction of $U_2$. The first velocity is nearly equal to the moving velocity $U_2$ because the inclination angle $\alpha$ between the journal and bearing is very small ($U_2$ is approximately $U_j$). The second velocity is derived from $U_2$ and $\alpha$ and written as

$$\frac{\partial}{\partial x}\left(h^3\frac{\partial p}{\partial x}\right)+\frac{\partial}{\partial z}\left(h^3\frac{\partial p}{\partial z}\right)=6\eta\left[(U_1-U_2)\frac{\partial h}{\partial x}+2\left(V_j+\frac{\partial h}{\partial t}\right)\right] \tag{3.1}$$

The direction of $V_j$ is negative and perpendicular to the oil film. The incompressible oil is squeezed thus increasing the oil film pressure [18].
Using Reynolds and continuity equation for the incompressible oil film in the wedge of the bearing, the pressure distribution in the oil film results as

$$\frac{\partial}{\partial x}\left(h^3\frac{\partial p}{\partial x}\right)+\frac{\partial}{\partial z}\left(h^3\frac{\partial p}{\partial z}\right)=6\eta\left[(U_1-U_2)\frac{\partial h}{\partial x}+2\left(V_j+\frac{\partial h}{\partial t}\right)\right] \tag{3.2}$$

where $p(x,z)$ is the oil film pressure; $h(x,t)$ is the oil film thickness; t is time; $\eta$ is the oil dynamic viscosity.

Substituting, one obtains the Reynolds lubrication equation.

$$\frac{\partial}{\partial x}\left(h^3\frac{\partial p}{\partial x}\right)+\frac{\partial}{\partial z}\left(h^3\frac{\partial p}{\partial z}\right)=6\eta\left[(U_1+U_2)\frac{\partial h}{\partial x}+2\frac{\partial h}{\partial t}\right] \tag{3.3}$$

We further simplify our problem, we use the isoviscous approximation of the Reynolds equation. This makes the assumptions that: steady state, constant density, temperature,

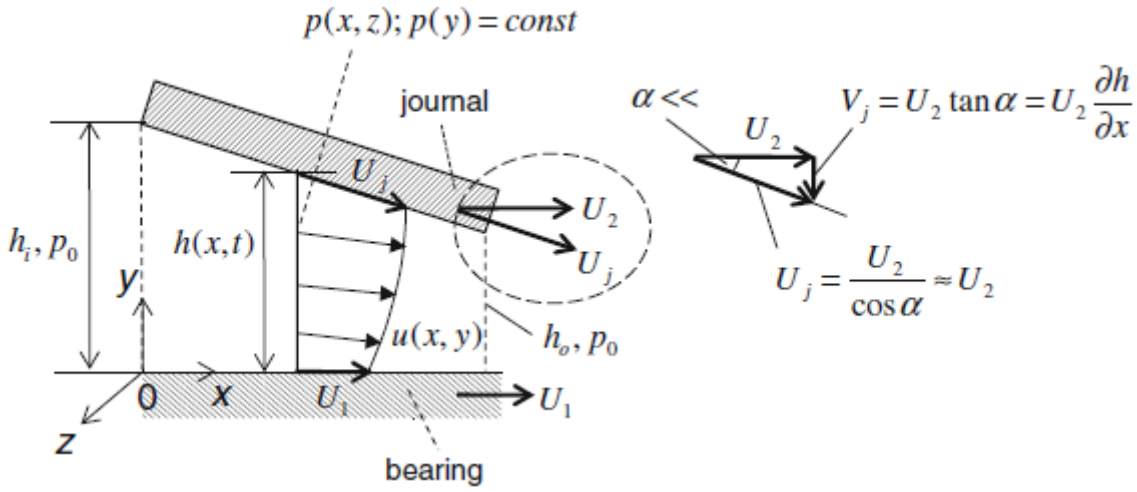


Figure 5: The Pressure distribution in thrust bearing
[20]

etc.

$$\frac{\partial}{\partial x}\left(h^3\frac{\partial p}{\partial x}\right)+\frac{\partial}{\partial z}\left(h^3\frac{\partial p}{\partial z}\right)=6\mu U\frac{dh}{dx} \tag{3.4}$$

There exist standard formulas with which the value of parameters necessary to solve the Initial Problem could be obtained.

- The length of the bearing pad, L:
  L = $R_1$ - $R_0$
- The tapered land width, B
  : B = $\frac{2\pi(R_0+R_1)}{2}$
- The convergence ratio, K:
  K = $\frac{B\tan\alpha}{h_0}$
- The Linear Velocity, U:
  U = $\frac{n\pi(R_0+R_1)}{60}$

### 3.2.1 Number of bearing pads

The number of pads in the thrust bearing of the turbocharger is given by:

$\phi_0 = 2\pi/n_p$

It is given in the initial problem that $\phi_0 = 60°$

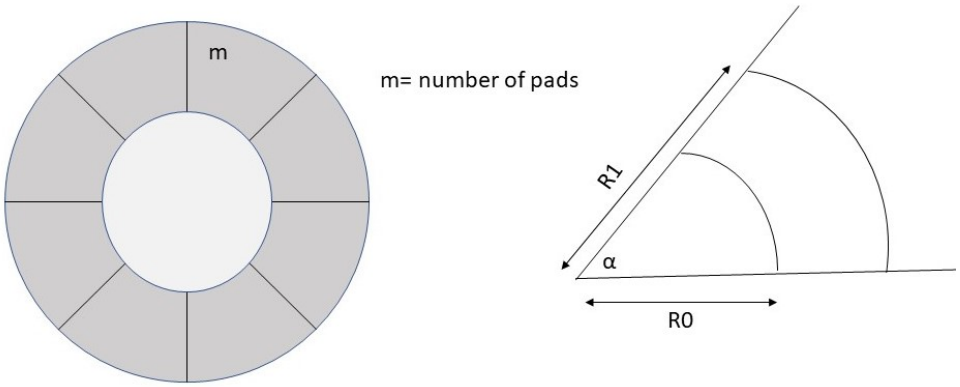


Figure 6: Parameters for designing the thrust bearing

Solving,we get that

$n_p = 6$

### 3.2.2 The Bearing Geometry

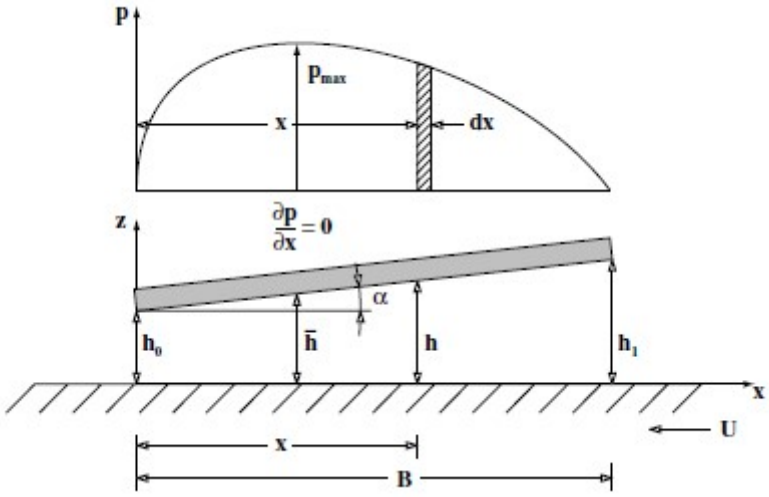


Figure 7: Bearing Geometry
[18]

As a result of the nature of the bearing geometry, it is necessary that its design discretizes the lubricating gap. This includes the input and output regions, which often involves millions of cells for only one segment of the thrust bearing [9].

The bearing geometry, h = f(x) has to be defined. the film thickness h is expressed as

$$\begin{aligned} h &= h_0 + x \tan\alpha = h_0 + x\frac{h_1 - h_0}{B} \\ h &= h_0\left(1 + \frac{h_1 - h_0}{h_0}\frac{x}{B}\right) \end{aligned} \tag{3.5}$$

The film geometry can then be expressed as:

$$h = h_0 \left(1 + \frac{Kx}{B}\right) \tag{3.6}$$

where 'K' is the convergence ratio given by: $\frac{h_1 - h_0}{h_0}$

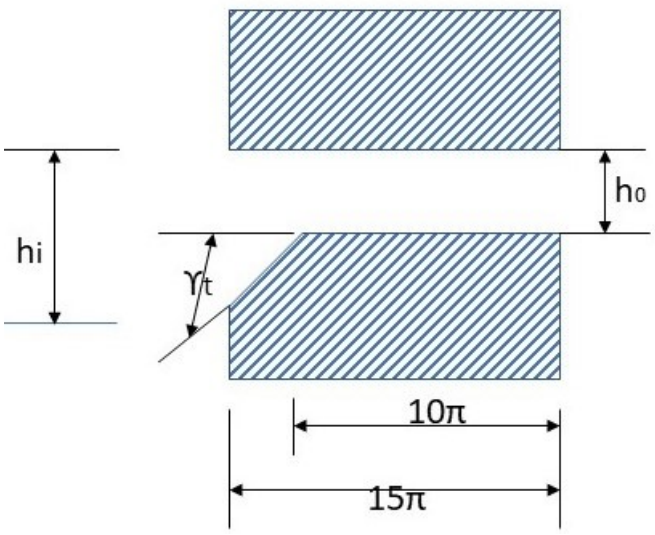


Figure 8: Parametrical description of Lub. Gap Geometry

**For the specific problem**

A parametrical description of the lubricating gap geometry can be given as:

$$h_i = h_0 + x \tan \gamma_t \tag{3.7}$$

where $x \in [10\pi, 15\pi] mm$ and $\gamma_t = 0.5^\circ$

$$h_i = h_0 + 0.00873x \tag{3.8}$$

### 3.2.3 Pressure distribution

The pressure distribution can be calculated by integrating the Reynolds equation over the special film geometry. Since the pressure gradient in the 'x' direction is dominant, the one-dimensional Reynolds equation for the long bearing approximation can be used for the analysis of this bearing. By differentiating which gives dx in terms

$$dx = \frac{B}{kh_0} dh \tag{3.9}$$

By proper substitution of equation(3.7), we obtain:

$$\frac{kh_0}{6U\eta B}dp = \frac{h-\bar{h}}{h^3}dh \tag{3.10}$$

which is the differential formula for pressure distribution in this bearing.

Integrating we get

$$\frac{kh_0}{6U\eta B}p = -\frac{1}{h} + \frac{\bar{h}}{2h^2} + C \tag{3.11}$$

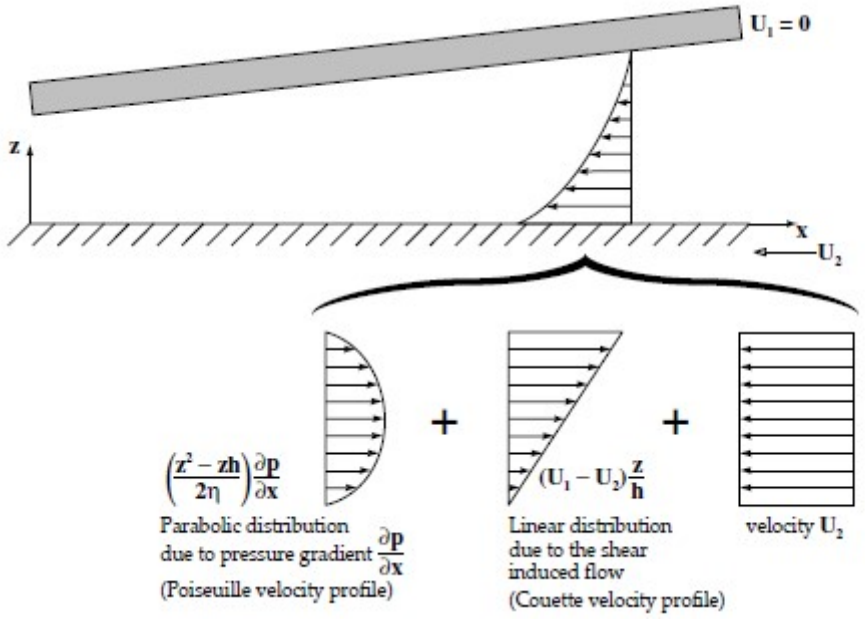


Figure 9: Velocity Profiles at entry of the hydrodynamic film [18]

With the boundary conditions according to *Figure*6 below

$$\begin{aligned} p &= 0 \quad \text{at} \quad h = h_0 \\ p &= 0 \quad \text{at} \quad h = h_1 \end{aligned} \tag{3.12}$$

Substituting the constants $'\bar{h}$ ' and ' C ' are:

$$\bar{h} = \frac{2h_0h_1}{h_1+h_0} C = \frac{1}{h_1+h_0} \tag{3.13}$$

From the convergence ratio ' K ', the maximum film thickness ' $h_1$ ' can be expressed in:

$$h_1 = h_0(K+1) \tag{3.14}$$

Substituting into the constants ' $\bar{h}$ ' and ' C ' in terms of ' K ':

$$\begin{aligned} \bar{h} &= 2h_0\frac{K+1}{K+2} \\ C &= \frac{1}{h_0(K+2)} \end{aligned} \tag{3.15}$$

Finally, substituting into equation (3.9) gives:

$$p = \frac{6U\eta B}{Kh_0}\left(-\frac{1}{h} + \frac{h_0}{h^2}\frac{(K+1)}{(K+2)} + \frac{1}{h_0(K+2)}\right) \tag{3.16}$$

### 3.2.4 Load Capacity

The total load that a bearing supports at a specific film geometry is obtained by integrating the pressure distribution over the specific bearing area. If the load is varied then the film geometry will change to re-equilibrate the load and pressure field. The load that the bearing will support at a particular film geometry is:

$$W = \int_0^L \int_0^B p dx dy \tag{3.17}$$

This can be re-written in terms of load per unit length:

$$\frac{W}{L} = \int_0^B p dx \tag{3.18}$$

$$\frac{W}{L} = \frac{6U\eta B}{Kh_0}\int_0^B \left(-\frac{1}{h} + \frac{h_0}{h^2}\frac{(K+1)}{(K+2)} + \frac{1}{h_0(K+2)}\right) dx \tag{3.19}$$

Substituting for dx and integrating yields:

$$\frac{W}{L} = \frac{6U\eta B^2}{K^2 h_0^2}\left(-\ln(K+1) + \frac{2K}{K+2}\right) \tag{3.20}$$

The total load per unit length the bearing will support expressed in terms of the bearing's geometrical and operating parameters which can be optimized to give the best performance.

### 3.2.5 Friction Force

According to [18], the friction force generated in the bearing due to the shearing of the lubricant is obtained by integrating the shear stress $\tau$ over the bearing area

$$F = \int_a^L \int_{\mathrm{a}}^{\mathrm{B}} T \ \mathrm{dedy} \tag{3.21}$$

The friction force per unit length is:

$$\frac{F}{L} = \int_0^B T dx \tag{3.22}$$

where shear stress is defined in terms of dynamic viscosity and shear rate:

$$\tau = \eta \frac{du}{dz} \tag{3.23}$$

where $du/dz$ is obtained by differentiating the velocity equation .In the bearing considered, the bottom surface is moving while the top surface remains stationary

$$U_1 = 0 \quad \text{and} \quad U_2 = U \tag{3.24}$$

thus the velocity equation is:

$$u = \left(\frac{\partial^2 - zh}{2\eta}\right)\frac{\partial p}{\partial x} - U\frac{z}{h} + U \tag{3.25}$$

Differentiating gives shear rate:

$$\frac{du}{dz} = (2z - h)\frac{1dp}{2\eta dx} - \frac{U}{h} \tag{3.26}$$

and substituting yields the friction force per unit length:

$$\frac{F}{L} = \int_0^B \left[\left(z - \frac{h}{2}\right)\frac{dp}{dx} - \frac{U_\eta}{h}\right]dx \tag{3.27}$$

The friction force on the lower moving surface, is greater than on the upper stationary surface. At the moving surface $x = 0$ (as shown, hence the net frictional force per unit length s

$$\frac{F}{L} = -\int_0^B \frac{h}{2}\frac{dp}{dx}dx - \int_0^B \frac{U_\eta}{h}dx \tag{3.28}$$

Integrating the first part of equation (3.26) by integration by parts: So if,

$$a = \frac{h}{2} \quad \text{and} \quad db = \frac{dp}{dx}dx \tag{3.29}$$

then

$$da = \frac{1}{2}dh \tag{3.30}$$

and

$$b = \int \frac{dp}{dx}dx = p \tag{3.31}$$

Substituting:

$$-\int_0^B \frac{h}{2}\frac{dp}{dx}dx = -\left(\left|\frac{h}{2}p\right|_0^B - \int_a^B \frac{1}{2}pdh\right) \tag{3.32}$$

the remaining term variables are replaced before integration and substituting for 'dh' in equation 3.7 gives:

$$-\int_0^B \frac{h}{2}\frac{dp}{dx}dx = 0 + \int_0^B \frac{1}{2}p\frac{Kh_0}{B}dx = \frac{Kh_0}{2B}\int_0^B pdx \tag{3.33}$$

Thus the first term of equation (3.26) is:

$$-\int_0^H \frac{h}{2}\frac{dp}{dx}dx = \frac{Kh_0}{B}\frac{W}{L} \tag{3.34}$$

And integrating the second term of equation

$$\int_0^B \frac{U_\eta}{h}dx = \frac{U_\eta B}{Kh_\mathrm{a}}[n(1 + K) \tag{3.35}$$

Then after substituting into equation the expression for friction force per unit length is obtained:

$$\frac{F}{L} = \frac{Kh_0}{2B}\frac{W}{L} - \frac{U_\eta B}{h_0 K}\ln(1 + k) \tag{3.36}$$

### 3.2.6 Coefficient of Friction

The coefficient of friction is expressed as a ratio of the friction and normal forces acting on the surface [18]:

$$\mu = \frac{\mathbf{F}}{\mathbf{W}} = \frac{\mathbf{F/L}}{\mathbf{W/L}} \tag{3.37}$$

substituting for F/L and W/L and simplifying:

$$\mu = \frac{\mathbf{Kh_0}}{\mathbf{B}} \left[ \frac{3\mathbf{K} - \mathbf{2}(\mathbf{K}+\mathbf{2})\ln(\mathbf{K}+\mathbf{1})}{6\mathbf{K} - \mathbf{3}(\mathbf{K}+\mathbf{2})\ln(\mathbf{K}+\mathbf{1})} \right] \tag{3.38}$$

### 3.2.7 Lubrication flow rate

Lubricant flow rate is an important design parameter. Sufficient quantity of lubricant must be supplied to the bearing to fully separate the surfaces by a hydrodynamic film. If the quantity of lubricant is supplied is in excess, then secondary frictional losses such as churning of the lubricant become significant. This effect can even overweigh the direct bearing frictional power loss. Precise calculation of lubricant flow is necessary to prevent overheating of the bearing from either lack of lubricant or excessive churning [18].

$$\mathrm{q_y} = 0 \tag{3.39}$$

Hence the lubricant flow in the bearing is obtained by integrating the flow per unit length $'\mathrm{q}'_\mathrm{x}$ over the length of the bearing:

$$\mathrm{Q_r} = \int_0^{\mathrm{L}} \mathrm{q}_x \, \mathrm{dy} \tag{3.40}$$

We know, from the equations describing the flow in a column that the flow rate in the x-direction is given by:

$$\mathrm{q_x} = -\frac{\mathrm{h}^3}{12\eta}\frac{\partial \mathrm{p}}{\partial \mathrm{x}} + (\mathbf{U}_1 + \mathbf{U}_2)\frac{\mathrm{h}}{2} \tag{3.41}$$

Substituting for ' $\mathbf{q}'_\mathrm{w}$ in the above equation :

$$\mathbf{Q_x} = \int_0^{\mathbf{L}} \left( -\frac{\mathbf{h}^3}{\mathbf{12}\eta}\partial\partial\mathbf{x} + \frac{\partial \mathbf{uh}}{\mathbf{2}} \right) \mathbf{dy} \tag{3.42}$$

The boundary conditions are: $\frac{dp}{dx} = 0$ at $h = \bar{h}$ (point of maximum pressure) substituting into (3.40) the flow is:

$$\mathbf{Q_x} = \int_0^{\mathrm{L}} \frac{\mathbf{U}\overline{\mathbf{h}}}{\mathbf{2}}\mathbf{dy} \tag{3.43}$$

substituting for $\overline{\mathrm{h}}'$ (eq. 3.13 ):

$$\mathbf{Q_x} = \int_0^{\mathbf{L}} \frac{\mathbf{U}}{\mathbf{2}}\mathbf{2h_0}\left(\frac{\mathbf{K}+\mathbf{1}}{\mathbf{K}+\mathbf{2}}\right)\mathbf{dy} \tag{3.44}$$

and simplifying yields the lubricant flow per unit length:

$$\frac{Q_\mathrm{J}}{\mathrm{L}} = \mathrm{Uh_0}\left(\frac{\mathbf{K}+\mathbf{1}}{\mathbf{K}+2}\right) \tag{3.45}$$

## 3.3 Numerical Solution of Reynolds Equation

This is the the substitution of all the real variables in the equation. It extends the generality of the numerical equation

### 3.3.1 Non-Dimesionalization of the Reynolds Equation

1. Hydrodynamic Pressure

   It is useful to find the pressure distribution in the bearing expressed in terms of bearing geometry and operating parameters such as the velocity ' U′ and lubricant viscosity ' $\eta$ '. A convenient method of finding the controlling influence of these parameters is to introduce non-dimensional parameters. In bearing analysis non-dimensional parameters such as pressure and load are used. Equation (3.15) can be expressed in terms of a nondimensional pressure, i.e.:

$$\mathrm{p}^* = \frac{\mathbf{h}_0}{\mathbf{K}}\left(-\frac{1}{\mathbf{h}} + \frac{\mathbf{h}_0}{\mathbf{h}^2}\frac{(\mathbf{K}+\mathbf{1})}{(\mathbf{K}+\mathbf{2})} + \frac{\mathbf{1}}{\mathbf{h_o}(\mathbf{K}+\mathbf{2})}\right) \tag{3.46}$$

   where the non-dimensional pressure $'\mathbf{p}^{*\prime}$ is:

$$\mathrm{p}^* = \frac{{\mathrm{h}_0}^2}{6\mathrm{U}\eta\mathrm{B}}\mathrm{p} \tag{3.47}$$

   Obviously, the hydrodynamic pressure is proportional to sliding speed ′U′ and bearing width ′B′ for a given value of dimensionless pressure and proportional to the reciprocal of film thickness squared.

2. Nondimensional Load Capacity
   In equation 3.18 above, it is the total load per unit length the bearing will support, expressed in terms of the bearing's geometrical and operating parameters. In terms of the non-dimensional load $'\mathbf{W}^{*\prime}$, equation 3.18 for the non-dimensional Reynolds equation can be expressed as:

$$\mathrm{W}^* = \frac{1}{\mathrm{K}^2}\left(-\ln(\mathbf{K}+1) + \frac{2\ \mathrm{K}}{K+2}\right) \tag{3.48}$$

   where:

$$\mathbf{W}^* = \frac{{\mathbf{h}_0}^2}{6\mathbf{U}\eta\mathbf{B}^2\mathbf{L}}\mathbf{W} \tag{3.49}$$

3. Frictional Force
   In a similar manner to load and pressure, frictional force is expressed in terms of the bearing's geometrical and operating parameters. In terms of the non-dimensional friction force $'\mathbf{F}''$ equation (3.34) is given by:

$$\mathrm{F}^* = \frac{6}{\mathrm{K}+2} - \frac{4\ln(\mathrm{K}+1)}{\mathrm{K}} \tag{3.50}$$

   where:

$$\mathbf{F}^* = \frac{\mathbf{h}_0}{\mathbf{U}\eta\mathbf{B}\mathbf{L}}\mathbf{F} \tag{3.51}$$

4. Coefficient of friction

   As was performed with load and friction, $\mu'$ can also be expressed in a so-called nondimensional or normalized form. In precise terms ' $\mu'$ is already non-dimensional but the purpose here is to find a general parameter which is independent of basic bearing characteristics such as load and size. Therefore ' $\mu'$ is defined entirely in terms of other nondimensional parameters:

$$\mu^* = \mathbf{K}\left[\frac{3\ \mathrm{K} - 2(\mathbf{K}+2)\ln(\mathbf{K}+\mathbf{1})}{6\mathbf{K} - 3(\mathbf{K}+2)\ln(\mathbf{K}+\mathbf{1})}\right] \tag{3.52}$$

   where:

$$\mu^* = \frac{\mathbf{B}}{\mathbf{h_0}}\mu \tag{3.53}$$

The Reynolds equation is expressed in terms of film thickness ' $\mathbf{h}'$, pressure ' $\mathrm{p}'$, entraining velocity ' $\mathrm{U}'$ and dynamic viscosity ' $\eta'$. Non-dimensional forms of the equation's variables are:

$$\begin{aligned} \mathrm{h}^* &= \tfrac{\mathrm{h}}{\mathrm{c}} \\ \mathrm{x}^* &= \tfrac{\mathrm{x}}{\mathrm{R}} \\ \mathrm{y}^* &= \tfrac{\mathrm{y}}{\mathrm{L}} \\ \mathrm{p}^* &= \tfrac{\mathrm{pc}^2}{6\mathrm{U}\eta\mathrm{R}} \end{aligned} \tag{3.54}$$

where: $\mathbf{h}$ is the hydrodynamic film thickness [m]; c is the bearing radial clearance [m]; $\mathbf{R}$ is the bearing radius [m]; $\mathbf{L}$ is the bearing axial length [m]; p is the pressure [Pa]; $\mathbf{U}$ is the bearing entraining velocity [m/s], i.e., $\mathrm{U} = (\mathrm{U}_1 + \mathrm{U}_2)/2$; $\eta$ is the dynamic viscosity of the bearing [Pas]; $\mathbf{x}, \mathbf{y}$ are hydrodynamic film co-ordinates [m]. The Reynolds equation in its non-dimensional form is:

$$\frac{\partial}{\partial \mathbf{x}^*}\left(\mathbf{h} * \frac{\partial}{\partial \mathbf{x}^*}\right) + \left(\frac{\mathbf{R}}{\mathbf{L}}\right)^2 \frac{\partial}{\partial \mathbf{y}^*}\left(\mathbf{h}^* \frac{\partial \mathbf{p}^*}{\partial \mathbf{y}^*}\right) = \frac{\partial \mathbf{h}^*}{\partial \mathbf{x}^*} \tag{3.55}$$

All terms in the above equation are non-dimensional apart from ' $\mathbf{R}'$ and ' $\mathbf{L}$ ' which are only present as a non-dimensional ratio[18].

### 3.3.2 The Vogelpohl Parameter

The Vogelpohl parameter ' $\mathbf{M_v}'$ is derived as follows:

$$\mathbf{M}_{\mathrm{v}} = \mathbf{p}^* \mathbf{h}^{*1.5} \tag{3.56}$$

Substitution into the non-dimensional form of Reynolds equation yields the 'Vogelpohl equation':

$$\frac{\partial^2 \mathbf{M}_{\mathrm{v}}}{\partial \mathbf{x}^* +}\left(\frac{\mathbf{R}}{\mathbf{L}}\right)^2 \frac{\partial^2 \mathbf{M}_{\mathrm{v}}}{\partial \mathbf{y}^*} = \mathbf{F}\mathbf{M}_{\mathrm{v}} + \mathbf{G} \tag{3.57}$$

where parameters ' $\mathrm{F}'$ and ' $\mathrm{G}'$ for journal bearings are as follows:

$$\begin{aligned} \mathbf{F} &= \frac{\mathbf{0.75}\left[\left(\frac{\partial \mathbf{h}^*}{\partial \mathbf{x}^*}\right)^2 + \left(\frac{\mathbf{R}}{\mathbf{L}}\right)^2 \left(\frac{\partial \mathbf{h}^*}{\partial \mathbf{y}^*}\right)^2\right]}{\mathbf{h}^{*2}} + \frac{\mathbf{1.5}\left[\frac{\partial^2 \mathbf{h}^*}{\partial \mathbf{x}^{*2}} + \left(\frac{\mathbf{R}}{\mathbf{L}}\right)^2 \frac{\partial^2 \mathbf{h}^*}{\partial \mathbf{y}^{*2}}\right]}{\mathbf{h}^*} \\ \mathbf{G} &= \frac{\left(\frac{\partial \mathbf{h}^*}{\partial \mathbf{x}^*}\right)}{\mathbf{h}^{*1.5}} \end{aligned} \tag{3.58}$$

The Vogelpohl parameter facilitates computing by simplifying the differential operators of the Reynolds equation, and furthermore it does not show high values of higher derivatives in the final solution, i.e., $d^n\mathbf{M}_v/dx^{*n}$ where $n > 2$, unlike the dimensionless pressure $p^{*\prime}$. This is because where there is a sharp increase in ' $p^{*\prime}$ close to the minimum of hydrodynamic film thickness ' $\mathbf{h}^{*\prime}, '\mathbf{M_v}'$ remains at moderate values. Large values of higher derivatives cause significant truncation error in numerical analysis.

### 3.3.3 Finite Difference Method

Journal bearing problems are usually solved by finite difference method. It is based on the approximation of a quantity by the difference between two function values at two or more adjacent nodes.

For example:

$$\left(\frac{\partial \mathbf{M_v}}{\partial \mathbf{x}^*}\right)_\mathbf{i} \approx \frac{\mathbf{M_{v,i+1}} - \mathbf{M_{v,i-1}}}{2\,\delta \mathbf{x}^*}$$

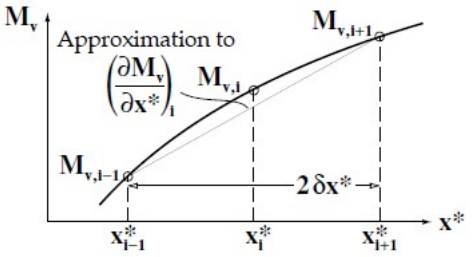


Figure 10: Position of Nodes in FD Equivalent of RE
[18]

where the subscripts $\mathbf{i}-1$ and $\mathrm{i}+1$ denote positions immediately behind and in front of the central position ' $\mathbf{i}'$ and $'\delta\mathbf{x}^{*\prime}$ is the step length between nodes. A similar expression results for the second differential $\partial^2\mathbf{M_v}/\partial x^{*2}$. This expression can be found according to the principle illustrated in Figure 5.2. The second differential $\partial^2\mathbf{M_v}/\partial\mathbf{x}^{*2}$ is found by subtracting the expression for $\partial\mathbf{M_v}/\partial\mathbf{x}^*$ at the $\mathrm{i}-0.5$ nodal position from the $\mathrm{i}+0.5$ nodal position and dividing by $\delta\mathrm{x}^*$, i.e.:

$$\left(\frac{\partial^2\mathbf{M}_v}{\partial\mathbf{x}^{*2}}\right)_1 \approx \frac{\left(\frac{\partial\mathbf{M}_v}{\partial\mathbf{x}^*}\right)_{1+0.5} - \left(\frac{\partial\mathbf{M}_v}{\partial\mathbf{x}^*}\right)_{1-0.5}}{\delta\mathbf{x}^*} \tag{3.59}$$

where:

$$\begin{aligned}\left(\frac{\partial\mathbf{M}_v}{\partial\mathbf{x}^*}\right)_{1+0.5} &\approx \frac{\mathbf{M}_{\mathrm{v},1+1}-\mathbf{M}_{v,1}}{\delta\mathbf{x}^*}\\ \left(\frac{\partial\mathbf{M}_v}{\partial\mathbf{x}^*}\right)_{1-0.5} &\approx \frac{\mathbf{M}_{\mathrm{v},1}-\mathbf{M}_{\mathrm{v},1-1}}{\delta\mathbf{x}^*}\end{aligned} \tag{3.60}$$

substituting into (4.5) yields:

$$\left(\frac{\partial^2\mathbf{M}_v}{\partial\mathbf{x}^*)}\right) \approx \frac{\mathbf{M}_{\mathrm{v},1+1} + \mathbf{M}_{\mathrm{v},1-1} - 2\mathbf{M}_{\mathrm{v,l}}}{\left(\delta\mathbf{x}^*\right)^2} \tag{3.61}$$

The finite difference equivalent of $(\partial^2\mathbf{M_v}/\partial x^{*2} + \partial^2\mathbf{M_v}/\partial \mathrm{y}^{*2})$ is found by considering the nodal variation of ' $\mathbf{M_y}'$ in two axes, i.e., the ' $\mathbf{x}'$ and ' $\mathbf{y}$ ' axes. A second nodal

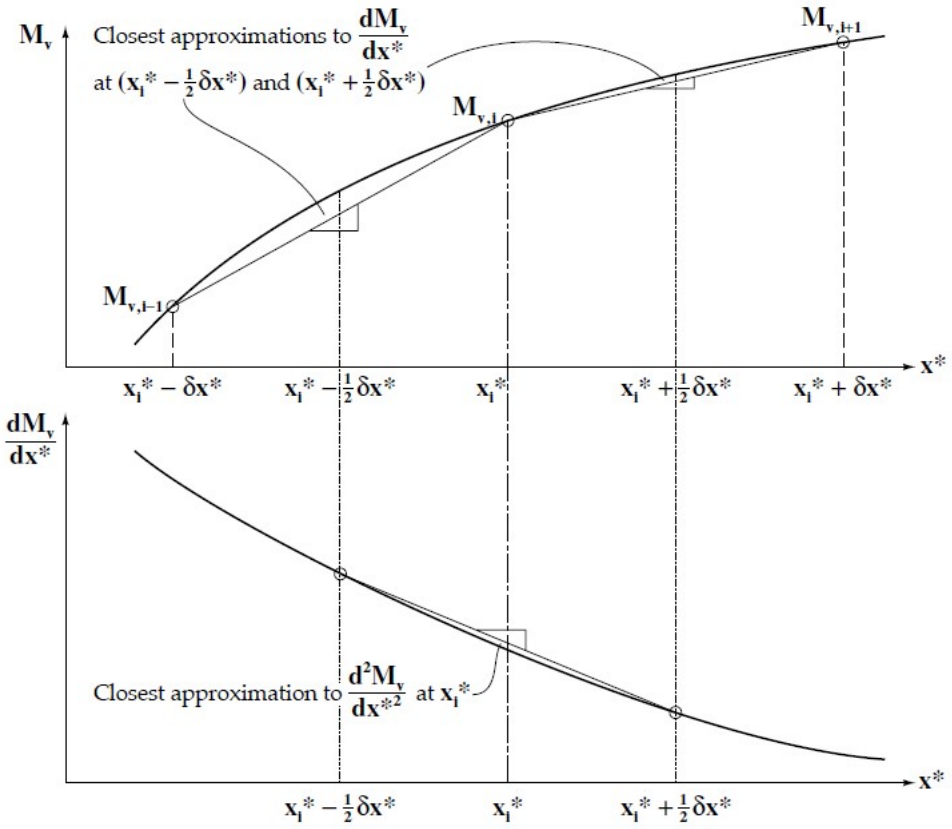


Figure 11: Illustration of FDA of second derivative function
[18]

position variable is introduced along the ' y ' axis, the ' j ' parameter. The expressions for $\partial \mathbf{M_v}/\partial y^*$ and $\partial^2 \mathbf{M_v}/\partial \mathbf{y}^{*2}$ are exactly the same as the expressions for the ' x′ axis but with 'i' substituted by ' j′. The coefficients of ' $\mathbf{M_v}'$ at the ' $\mathbf{i}'$ -th node and adjacent nodes required by the Reynolds equation which form a 'finite difference operator' are usually conveniently illustrated as a 'computing molecule'[18].

The finite difference operator is convenient for computation and does not create any difficulties with boundary conditions. When the finite difference operator is located at the boundary of a solution domain, special arrangements may be required with imaginary nodes outside of the boundary. There are more complex finite difference operators available based on longer strings of nodes but they are rarely used despite their greater accuracy [18]. The terms 'F′ and ' G′ can be included with the finite difference operator to form a complete equivalent of the Reynolds equation. The equation can then be rearranged to provide an expression for $\mathbf{M}_{\mathrm{v},1,1}'$ i.e.:

$$\mathbf{M}_{\mathrm{v,1,j}} = \frac{\mathbf{C}_1 \left(\mathbf{M}_{\mathrm{v},+1,1} + \mathbf{M}_{\mathrm{v},1-1,j}\right) + \left(\frac{\mathbf{R}}{\mathbf{L}}\right)^2 \mathbf{C}_2 \left(\mathbf{M}_{\mathrm{v},.,\mathrm{j}+1} + \mathbf{M}_{\mathrm{v},1,51}\right) - \mathbf{G}_{\mathrm{i,J}}}{2\mathbf{C}_1 + 2\mathbf{C}_2 + \mathbf{F}_{1,\ \mathrm{J}}} \tag{3.62}$$

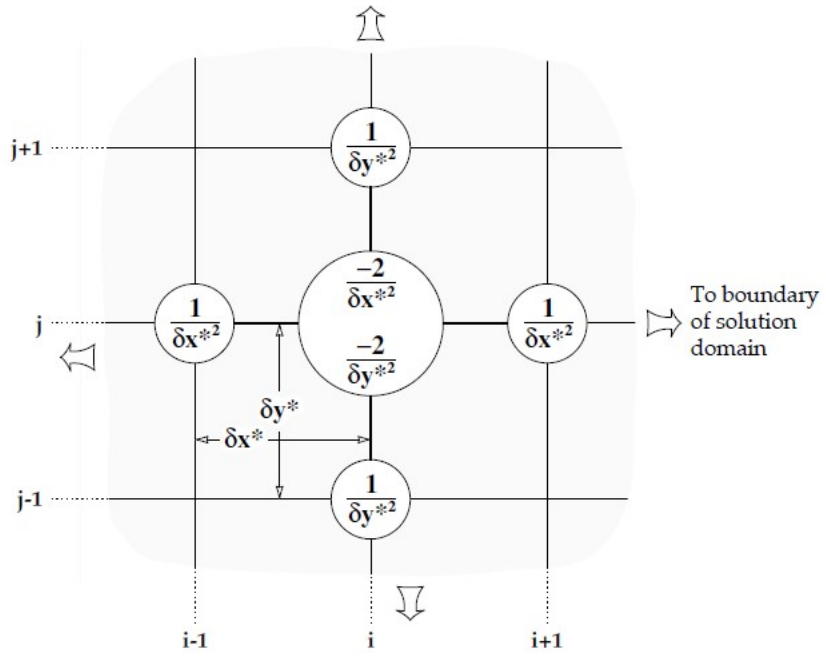


Figure 12: FD operator and nodal scheme for numerical analysis of RE [18]

where:

$$C_1 = \frac{1}{\delta x^{*2}}$$
$$C_2 = \frac{1}{\delta y^{*2}}$$

This expression forms the basis of the finite difference method for the solution of the Reynolds equation. Its solution gives the required nodal values of ' $\mathbf{M_v}'$. [1]

## 3.4 Newton's Method

Newton's method is one of the most powerful and widely-used methods of solving f(x)=0. It originates from the Taylor series expansion of f(x) about the point x.

Starting with an initial guess $x_0$, we can find the value of $f(x_0)$ then approximate the graph of f by suitable tangents. With the approximate value $x_0$ got from the graph of f, $x_1$ being the intersection of the x-axis and the tangent of the curve of f at $x_0$

$$\begin{aligned} \tan\theta_0 = f'(x_0) &= \frac{f(x_0)}{x_0 - x_1} \\ \Rightarrow x_1 &= x_0 - \frac{f(x_0)}{f'(x_0)} \end{aligned} \tag{3.63}$$

From this the Newton iteration formula can be written in the form:

$$x_{n+1} = x_n - \frac{f(x_n)}{f'(x_n)} \tag{3.64}$$

[1] The contents of the section on Splines are referenced from the book "Engineering Tribology Third Edition" by STACHOWIAK, Gwidon W. a Andrew BATCHELOR. which is also listed in the Bibliography section[18]

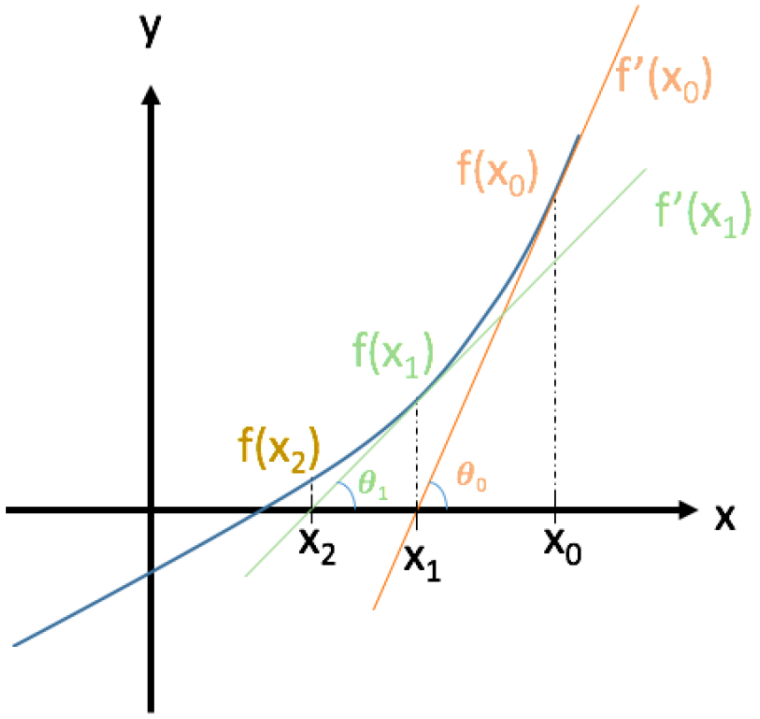


Figure 13: Newton-Raphson Method
[26]

It is worthy to note that the Newton's method has some drawbacks in finding the derivative terms . This led Leong et al [17] to present the possibility of using the Jacobian while using Newton's method.

## 3.5 Shapes and Splines

### 3.5.1 Shape Optimization

Shape optimization is a very integral part of design and construction. For example, if an aircraft is to be marked safe to use, there are criteria on mechanical performance it must satisfy while weighing as little as possible.

"The shape optimization problem for structures like the aircraft consists in finding a geometry of the structure which minimizes a given functional (e.g. such as the weight of the structure) and yet simultaneously satisfies specific constraints (like thickness, strain energy, or displacement bounds). The geometry of the structure can be considered as a given domain in the three-dimensional Euclidean space. The domain is an open, bounded set whose topology is given, e.g. it may be simply or doubly connected. The boundary is smooth or piecewise smooth, so boundary value problems that are defined in the domain and associated with the classical partial differential equations of mathematical physics are well posed. [32]"

Generally, the objective function (cost functional), takes the form of an integral over

the domain or its boundary where the integrand depends smoothly on the solution of a boundary value problem.

The shape optimization problem then involves the minimization of such a functional with respect to the geometrical domain which must belong to the admissible family, the set of admissible solutions.

To solve a shape optimization problem is to find the minimum - whenever it exists - of a specific cost functional over a set of admissible domains. However, very few adequate results exist. The existence of the results for these problems are obtained, provided that some constraint, mostly unrealistic, are imposed on the family of admissible domains [32].

### 3.5.2 Splines

Splines are piecewise polynomial curves that are differentiable up to a prescribed order.

A curve s($u$) is called a spline of degree $n$ with the knots $a_0, \ldots, a_m$, where $a_i \leq a_{i+1}$ and $a_i < a_{i+n+1}$ for all possible $i$, if

s($u$) is $n-r$ times differentiable at any $r$ -fold knot[1], and s($u$) is a polynomial of degree $\leq n$ over each knot interval $[a_i, a_{i+1}]$, for $i = 0, \ldots, m-1$

It is also common to refer to a spline of degree $n$ as a spline of order $n+1$.

**Properties of B-Splines**

- The B-splines of degree $n$ with a given knot sequence that do not vanish over some knot interval are linearly independent over this interval.

- A dimension count shows that the B-splines $N_0^n, \ldots, N_m^n$ with the knots $a_0, \ldots, a_{m+n+1}$ form a basis for all splines of degree $n$ with support $[a_0, a_{m+n+1}]$ and the same knots.

- Similarly, the B-splines $N_0^n, \ldots, N_m^n$ over the knots $a_0, \ldots, a_{m+n+1}$ restricted to the interval $[a_n, a_{m+1})$ form a basis for all splines of degree $n$ restricted to the same interval.

- The B-splines of degree $n$ form a partition of unity, i.e.

$$\sum_{i=0}^{m} N_i^n(u) = 1, \quad \text{for} \quad u \in [a_n, a_{m+1})$$

- A spline $\mathbf{s}\,[a_n, a_{m+1}]$ of degree $n$ with $n$ -fold end knots, $(a_0 =)\, a_1 = \ldots = a_n$ and $a_{m+1} = \ldots = a_{m+n}\,(= a_{m+n+1})$ has the same end points and end tangents as its control polygon.

- The end knots $a_0$ and $a_{m+n+1}$ have no influence on $N_0^n$ and $N_m^n$ over the interval $[a_n, a_{m+1}]$.

- The B-splines are positive over the interior of their support,

$$N_i^n(u) > 0 \quad \text{for} \quad u \in (a_i, a_{i+n+1})$$

- The B-splines have compact support,

$$\operatorname{supp} N_i^n = [a_i, a_{i+n+1}]$$

- The B-splines satisfy the de Boor, Mansfield, Cox recursion formula

$$N_i^n(u) = \alpha_i^{n-1} N_i^{n-1}(u) + \left(1 - \alpha_{i+1}^{n-1}\right) N_{i+1}^{n-1}(u)$$

  where $\alpha_i^{n-1} = (u - a_i) / (a_{i+n} - a_i)$ represents the local parameter over the support of $N_i^{n-1}$.

- The derivative of a single B-spline is given by

$$\frac{d}{du} N_i^n(u) = \frac{n}{u_{i+n} - u_i} N_i^{n-1}(u) - \frac{n}{u_{i+n+1} - u_{i+1}} N_{i+1}^{n-1}(u)$$

- The B-spline representation of a spline curve is invariant under affine maps.

- Any segment $\mathbf{s}_j\,[a_j, a_{j+1})$ of an $n$ th degree spline lies in the convex hull of its $n+1$ control points $\mathbf{c}_{j-n}, \ldots, \mathbf{c}_j$

For these properties, the splines would be used to generate a working lubricating gap profile for the always-varying lubricating gap of the tilting-pad thrust bearing. [2]

## 3.6 Genetic Algorithm

### 3.6.1 Introduction

Many problems of science are solved by imitating nature, many insights that have advanced science have come from this process. Genetic algorithm is the computational adaptation of the evolution process. Specifically, it attempts to replicate Lamarck's process of natural selection.

The genetic algorithm is a kind of evolutionary algorithm. Evolutionary algorithms first construct an initial population, then reiterates through three procedures:

i Fitness evaluation: The fitness of the individuals in the population is evaluated. Members of the population are stochastically selected based on their fitness.

[2] The contents of this section on Splines are all referenced from the book Bezier and B-Splines techniques listed in the Bibliography section [33]

ii Breeding: the selected individuals form the parent population. They then breed among themselves to produce offspring.

iii Crossover and mutation: the members of the parent population are selected randomly and modified. The offspring population is subjected to fitness evaluation and stochastically selected for breeding with each other and/or with selected members of the parent population.

Then this process is repeated until a certain condition is satisfied.

Genetic algorithms are multi-directional search, derivative-free stochastic search algorithms that apply the idea of natural selection.

One of the many difficulties in engineering design and multi-objective optimization is meeting the robustness requirement. Genetic algorithms are being extensively applied to engineering problems because they can locate pareto front. The pareto front is a set of reduced actions. It is derived after weaker solutions, solutions that are easily dominated by most other solutions in the set of solutions, have been removed or taken away from the set of solutions.

Dominance ranks are used to push the population close to the pareto front. With larger population there is the tendency to be more localized in the search for an optimal result. For a more robust solution, it is good allow for diversity. It is common knowledge that in industry, most times, robustness of solutions sometimes trump optimality. Therefore, to allow for robustness of solution and to get some 'control of the population', diversity must be adapted into this search algorithm. Though paradoxical, the goal is to attain convergence and diversity.

**Advantages of Genetic Algorithm**

- It is robust; has a wide range of applications.
- It can be directly implemented in optimization tools and packages.
- It is easy to deal with discrete design variables.
- It is useful in finding global solution of multivariate objective function.
- It effortlessly captures multiple non-inferior solutions.
- It uses probabilistic and not deterministic operators.
- It is less likely to be trapped in a local minimum.
- Provides local and global solution.
- In many cases, they are less sensitive to the presence of noise and uncertainty in measurements.

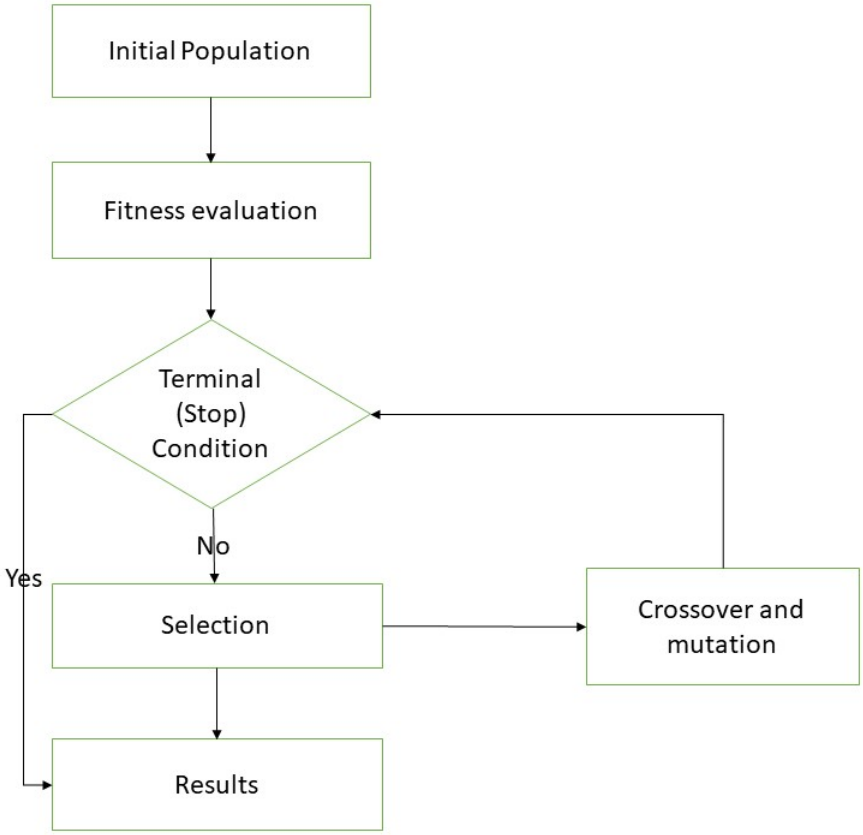


Figure 14: Flowchart for Genetic Algorithm

**Disadvantages of Genetic Algorithm:**

- It requires comparatively less information about the problem.

- It is computationally time consuming. A single solution of a bearing steady state may include hours of computational time on high-performance computers. This fact makes it practically impossible to use these calculations for multiple repetitive tasks involving the solution of hundreds or thousands of operating states.

### 3.6.2 Adaptation of the Genetic Algorithm to our problem

"GA problematics use standard terminology: an individual, a gener- ation, a gene, an objective function or a fitness function. Thrust bear- ing integral characteristics, as a result of the numerical solution of the lubricant flow and heat transfer, are used to search for the optimal pa- rameters of a thrust bearing. Each solution (marked as an individual) is represented by a set of variables (marked as genes) and is evaluated us- ing integral characteristics (marked as the objective function). To create a new generation, the fitness function is calculated for each individual, based on the objective function. The algorithm thus searches for the global minimum of the objective function, depending on the genes. In this case, the fitness function is expressed as a negative value of the objective function and expresses the quality of the thrust bearing design represented by the individual.

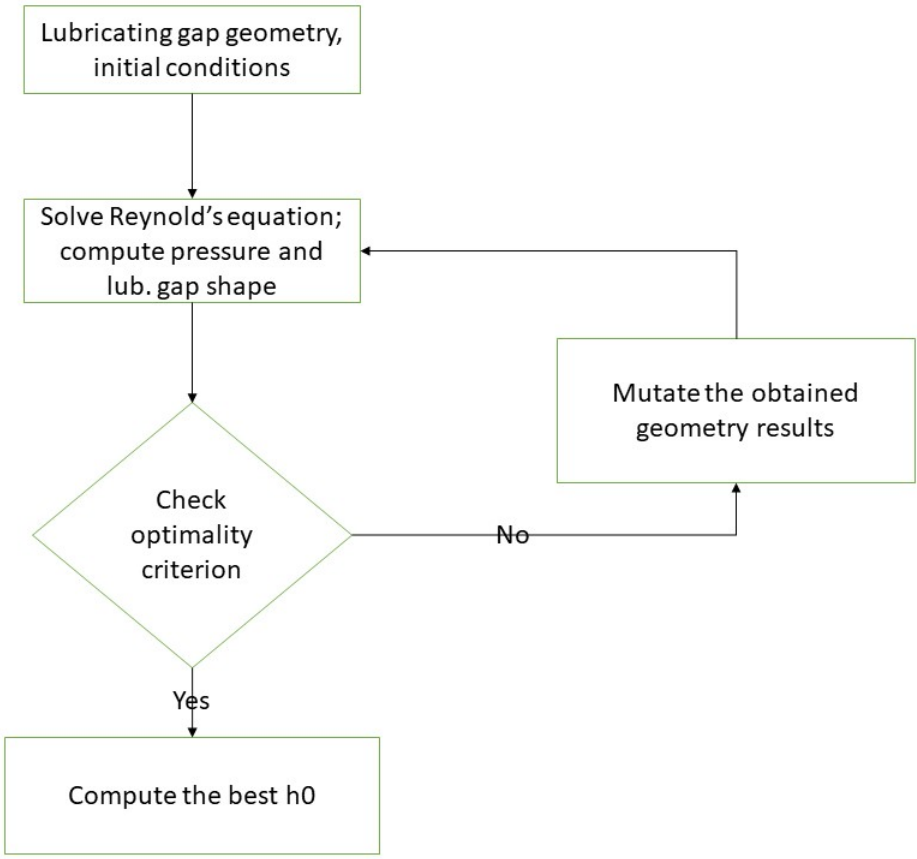


Figure 15: Flowchart for Adapted Genetic Algorithm

Individuals are stochastically selected and modified by the genetic operators, including a selection, a crossover and a mutation.

After the application of these genetic operators, a new generation is created. The proposed strategy includes a generation model of GA constrained by the limit values of genes and elitism. In this model, a new generation of individuals is created with each iteration, while a predetermined pro- portion of the best individuals (referred to as elite individuals) from the previous generation is maintained [8]."

The initial problem, as discussed earlier, is an Optimization problem.

The problem, as written in Section 1.3, where it is stated that: The criteria under which the problem is to be solved:

i Minimize friction force.

ii Maintain load capacity.

iii Do not increase lubrication flow rate.

iv Do not decrease minimum gap thickness.

This is a Multi Objective Optimization Problem. From 3.36, 3.19 and 3.45

**Objective I:** Minimize friction force

$$F = \frac{LU\eta B}{h_0}\left(\frac{6}{(K+2)} - \frac{4\ln(K+1)}{K}\right) \tag{3.65}$$

**Objective II:** Maintain Load Capacity

The Load capacity is given by equation(3.19).

$$W = \frac{6LU\eta B^2}{K^2 h_0^2}\left(-\ln(K+1) + \frac{2K}{K+2}\right) \tag{3.66}$$

The given load capacity from the initial problem is 100N. This means that this load capacity is to be maintained.

**Objective III:** Do not increase lubrication flow rate
The lubrication flow rate, equation (3.43), is given by:

$$\frac{Q_{\mathrm{J}}}{\mathrm{L}} = \mathrm{Uh}_0\left(\frac{\mathbf{K+1}}{\mathbf{K+2}}\right) \tag{3.67}$$

Hence, the lubrication flow rate, as a constraint, is given by:

$$\frac{Q_{\mathrm{J}}}{\mathrm{L}} \lessapprox \mathrm{Uh}_0\left(\frac{\mathbf{K+1}}{\mathbf{K+2}}\right) \tag{3.68}$$

**The Constraint:** Do not decrease minimum lubricating gap thickness.

# 4 Results and Discussions

## 4.1 Introduction

The initial problem, Section 1.3, was solved using formulae from the Materials and Methods section. The computed results are shown and discussed in the following subsections.

## 4.2 Pressure Distribution

Using the non-dimensional parameters, the non-dimensional pressure distribution that solves the Reynolds equation for this setup (system) was computed. The numerical version of the Reynolds equation, was computed using Finite Difference Method.

The non-dimensional pressure for the initial problem was calculated using MATLAB. The mesh was of size 50x50. The codes are in the Appendix.

The value for the peak non-dimensional pressure is 0.05489.

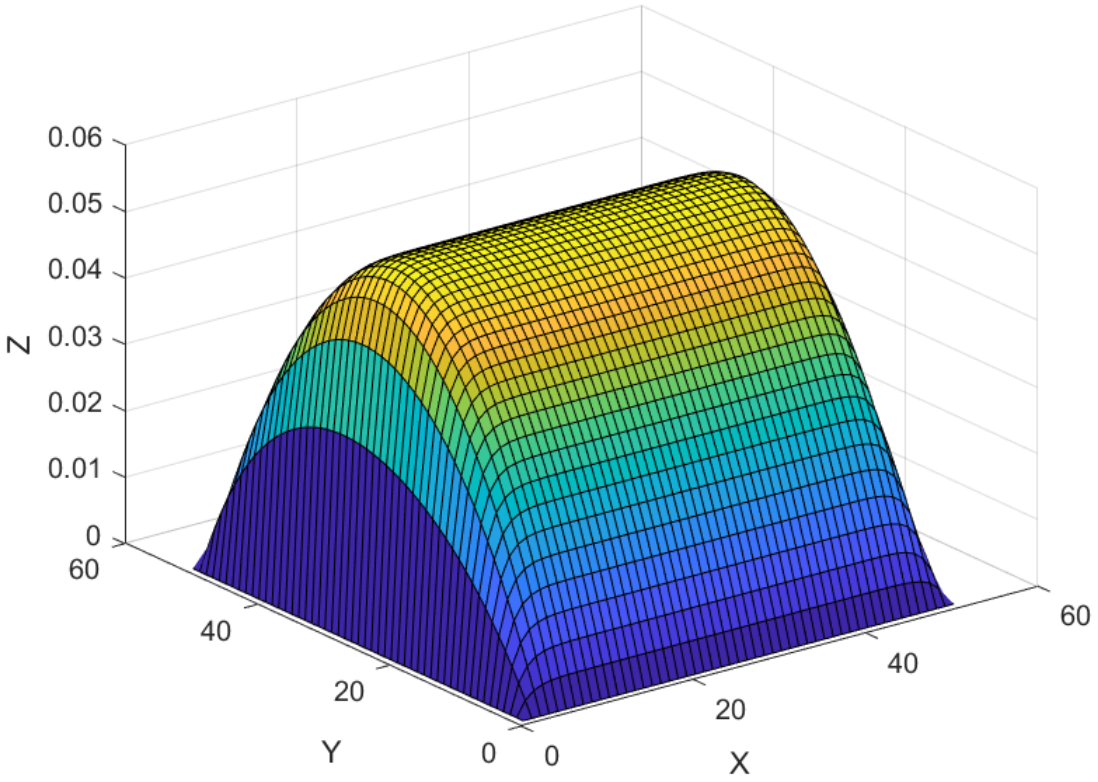


Figure 16: Nondimensional Pressure Distribution

Using the formula showing the relationship between the non-dimensional pressure and the pressure:

$$p^* = \frac{{h_0}^2}{6U\eta B}p \tag{4.1}$$

The peak pressure can be obtained for the initial problem.

$p = 148857.8124 N/m_2$

$p \approx 14.9 Pa$

## 4.3 Initial Lubrication Gap Size

Use the already discussed Newton's methods (Section 3.3). The Newton-Raphson method is applied in MATLAB. We take an initial guess of 0.0005, making sure that we do not go below the recommended minimum gap thickness of 20-50 micrometers.

The problem of initial geometry for the lubrication gap was using Newton's Method in MATLAB. The codes can be found in the Appendix section.

The Jacobian can be applied to assist the Newton's method. Some of the downsides of the Newtons method can be glossed over with the Jacobian method.[26]

**Applying Jacobian to Newtons Method**

It is necessary to find the derivative terms given by equation(3.62)

$$x_{n+1} = x_n - \frac{f(x_n)}{f'(x_n)}$$

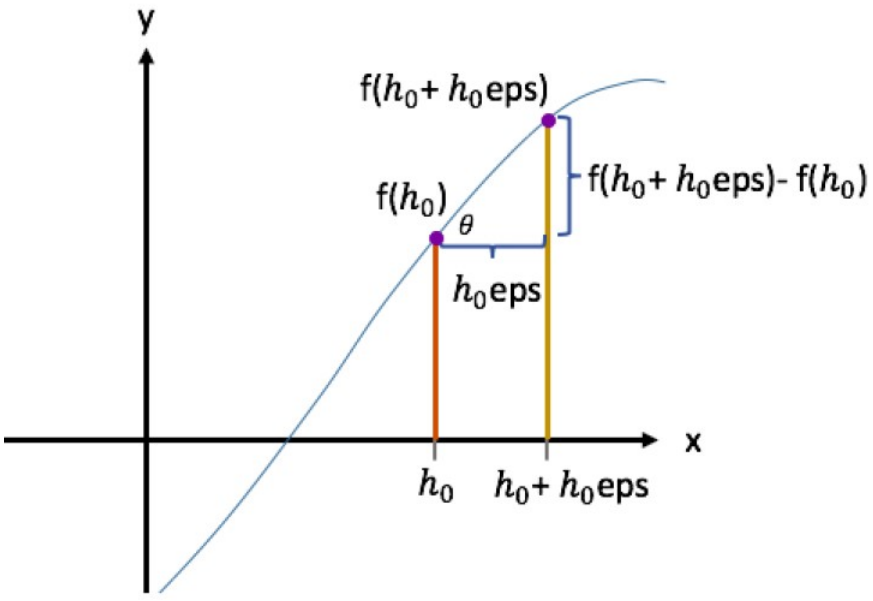


Figure 17: Newton Method with Jacobian
[26]

From the above figure, it is apparent that:

$$\tan\theta = \frac{f\left(h_0 + h_0 eps\right) - f\left(h_0\right)}{h_0 eps} \tag{4.2}$$

The model in the Appendix is computed in the following way:

1. It starts off with the initial guess of $h_0 = 0.0005$. The convergence ratio K is then computed with this initial $h_0$

2. With the given load, W, and $h_0$, we compute the difference $f = f(h_0) - W$ .

3. The change in x, $\triangle x$ is $h_0 epps$. With this value, we recompute the difference $ff = f(h_0 + eps) - W$

4. Equate the jacobian to $(ff - f)/h_0 eps$ ; this coincides with tan$\theta$ in the figure above.

5. For the next iteration of $h_0$ is computed by $h_0 = h_0 - 0.0009.f/jacobian$

6. Comparing the two values f and W, we take a ratio of both of them. To adjust for errors, we repeat the calculation until the error is less than 1e-4, i.e. the approximation point is closed or almost equal to the root answer [26].

The initial geometry for the problem was obtained to be 0.0004695 m $\approx$ 0.45mm.

The significance of this initial geometry, thus obtained, is to serve as a benchmark for the possible solutions to be obtained from the Genetic Algorithm. The optimal value should be:

$$h_{opt} < 0.0004695m \tag{4.3}$$

is then used as a constraint in solving the Geometric Algorithm.
The standard expectation of the minimum lubricating gap thickness is: $h_0 \geq 0.000003m$. By this standard, the value obtained from 4.3 is in the clear.

## 4.4 Initial Solution to Optimization Problem

Solving 3.36, 3.19, 3.45 and the equations of necessary parameters, the following values were obtained:

| Parameters | Values |
|---|---|
| $R_0$ | 0.03m |
| $n_p$ | 6 |
| $R_1$ | 0.06m |
| $\eta$ | 0.001Pas |
| n | 45000rpm |
| $h_0$ | 0.0004695 m |
| U | 212.06 m/s |
| B | 0.4712 |
| K | 0.0041 |
| L | 0.03m |
| $Q_0$ | 0.0015 $m^3/s$ |
| $F_0$ | -63.72 N |
| $W_0$ | -130.94N |

## 4.5 Initial Gap Profile

The problem is to describe a general lubricating gap profile. This general lubricating gap profile is also called initial gap profile in this work. It is created by a general function, arbitrarily. For this work, it is described by a spline function.

### 4.5.1 Spline Function

To do this, it is necessary to find the optimal lubricating gap size for 100 points; we have to iterate a hundred times in the GA.

Calculating for the lubricating gap size for one hundred points is a tedious job;it will take a lot of computational time and one is bound to make heinous errors.

To simplify the problem, we define a spline function to describe the lubricating gap profile. With this, we can obtain control points. The size of the lubricating gap is calculated for the analytically for the initial point.

### 4.5.2 Control Points

The control points are the points marked '*' in the Fig.18.

These control points were chosen arbitrarily and the gap profile was computed in MATLAB using the Spline function.

| Relative Position | Film thickness |
|---|---|
| X(0) = 0.0 | H(0) = 1.00 |
| X(1) = 0.5 | H(1) = 1.05 |
| X(2) = 0.1 | H(2) = 1.2 |

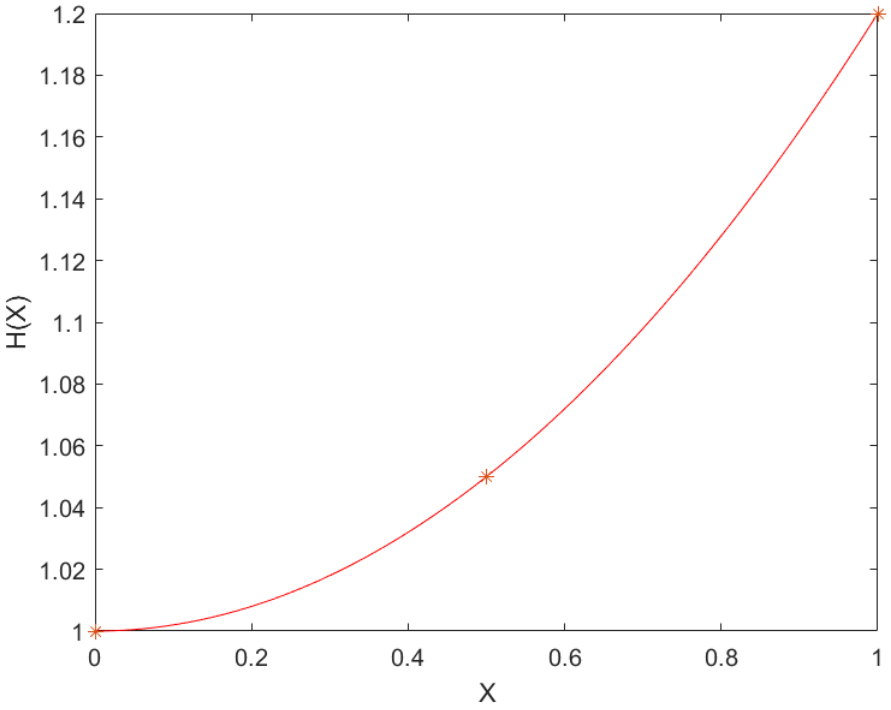


Figure 18: Spline Function with three control points defining a general profile

### 4.5.3 Reconstruction of Objective function

Considering that the problem is a multiobjective function, the objective function to be minimized is given as:

$$f_{\text{obj}}(\mathbf{x}) = \frac{\sum_{k=1}^{\max} f_{\text{f},k} s_{\text{m},k} s_{\text{w},k} s_{\text{h},k} w_k}{\sum_{k=1}^{k_{\max}} w_k} \tag{4.4}$$

where k reflects the number of operating conditions, in this case, the various control points, the initial bearing design $x_{init}$ is the initial parent vector and $w_k$ is the weighting factor selected depending on the operating conditions of the bearing. [8]

**The General Idea** is that for each parameter to be optimized, its formula is kept in the equation while the other 'factor' of the objective functions is used to multiply the objective function being minimized.

The friction torque ratio ($f_f$) is proposed relative to the friction torque of the initial bearing design($M_{f,init}$) under the considered operating condition of the form:

$$f_{\text{f}} = \frac{M_{\text{f}}}{M_{\text{f,init}}} \tag{4.5}$$

The mass flow rate factor increases the value of the objective function in this case where we have an upper-limit to the increase of lubricant flow rate; "Do not increase

lubricant flow rate."

$$s_{\mathrm{m}} = \max\left(1, \left(\frac{\dot{m}_{\mathrm{r}}}{\beta_m \dot{m}_{\mathrm{r,init}}}\right)^{\lambda}\right) \tag{4.6}$$

where $\beta_m \geq 1$. The factor $\beta_m = 2$ was chosen. This factor increases the tolerable mass flow rate and $\lambda \geq 1$ is a power exponent In his work, Novotný et al [8] suggests that a reasonable number for $\lambda = 3$.

The thickness factor increases the value of the objective function if it falls below the limit value ($h_{lim}$). The thickness factor is defined as follows:

$$s_{\mathrm{h}} = \max\left(1, \left(\frac{h_{\mathrm{lim}}}{h_{\mathrm{min}}}\right)^{\lambda}\right) \tag{4.7}$$

While the load capacity factor increases the value of the objective function highly. The load capacity factor is defined as follows:

$$s_{\mathrm{w}} = \max\left(1, \left(\frac{W_{\mathrm{i}}}{W_{\mathrm{init}}}\right)^{\lambda}\right) \tag{4.8}$$

These value for these factors were computed at the control points. The following results were obtained:

**For our specific problem**, since the goal is to solve for the value of the entire profile, the weighting factor is not to be used. Equation (4.7) is then modified to obtain:

$$f_{obj} = f_f s_w \tag{4.9}$$

The number of factors multiplied to obtain this simplified form of the equation is kept as little as possible. It is also necessary that the value of the objective function is $\approx 1$, i.e. it is the neighbourhood of 1.

This is to ensure that the specified conditions for optimization are met.

The Numerical solution of the Reynolds Equation was computed using MATLAB. The codes were written from the equations for the Finite Difference Method prescribed in Section 3.3.

The Vogelpohl parameter was computed and used to obtain the nondimensional pressure. The value of the nondimensional pressure was then used to obtain the pressure.

The procedure followed to write the codes are outlined in [18]. The MATLAB codes are in the Appendix section of this work.

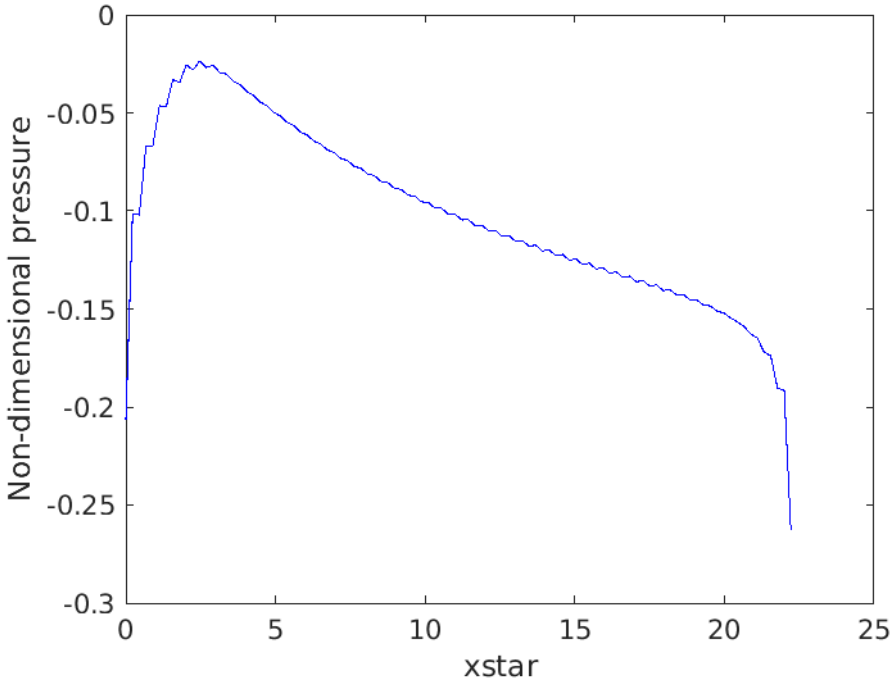


Figure 19: 2D Pressure distribution of working profile

The byproducts of the pressure obtained were The Load Capacity of the profile, the friction force and the lubricant flow rate.

Novotný et al in their paper [9] give the formulas for these "byproducts" and they are replicated below:

- **Friction force**
  $F_\mathrm{p}$ is the friction torque component due to the pressure gradient in the circumferential direction:

$$F_\mathrm{p} = n_\mathrm{s} \frac{h_0 R_1^2 p_\mathrm{b}}{2} h_\alpha h_\beta \sum_{i=1}^{m} \sum_{j=1}^{n} \left( \frac{\partial P_{i,j}}{\partial \beta_{i,j}} H_{i,j} \alpha_{i,j} \right) \tag{4.10}$$

- **Load Capacity**
  "$F_\mathrm{c}$ is the total bearing load capacity of all bearing segments and can be determined by numerical integration of quantities across the lubricating film as follows

$$F_\mathrm{c} = 2 n_\mathrm{s} \pi R_1^2 p_\mathrm{in}\, h_\alpha h_\beta \sum_{i=1}^{m} \sum_{j=1}^{n} P_{i,j} \alpha_{i,j} \tag{4.11}$$

  "

- **Mass flow rate**
  $\dot{m}_\mathrm{p}$ is the mass flow component caused by the pressure gradient in the radial direction and can be computed as:

$$\dot{m}_\mathrm{p} = -n_\mathrm{s} \frac{\pi h_0^3 p_\mathrm{b} \rho_{\mathrm{liq}\,0}}{6 \eta_{\mathrm{liq}\,0}} \frac{\bar{\rho}}{\bar{\eta}} h_\beta \sum_{j=1}^{n} \alpha_{m,j} H_{m,j}^3 \frac{\partial P_{m,j}}{\partial \alpha_{m,j}} \tag{4.12}$$

These formulas were used to improve upon the MATLAB codes written for section 3.3 of this work.

The following values were obtained numerically:

| **Relative Position** | **Film thickness** |
|---|---|
| $F_p$ | -134.9 N |
| $F_c$ | - 75 N |
| $\dot{m}_p$ | $m^3/s$ |

The factors were then calculated thus:

- **Friction factor**

$$f_f = \frac{Friction force_{numerical}}{Friction force_{analytical}}$$

- **Load capacity**

$$s_w = \frac{Load_{numerical}}{Load_{analytical}}$$

Substituting for the analytical values and numerical values:

$$f_f = \frac{Fr_{numerical}}{Fr_{analytical}} = \frac{-134.9}{-130} = 1.038$$

$$s_w = \frac{Fl_{numerical}}{Fl_{analytical}} = \frac{-75}{-63} = 1.19$$

Substituting in 4.9 we obtain:

$$f_{obj}(x) = 1.235 \tag{4.13}$$

## 4.6 GA Results

Following the preceding text of equation (4.9), the objective function, already computed above was optimized using GA in MATLAB. The codes can be found in the Appendix.

The optimal film thickness for the lubricant gap profile described by the spline function was found to be $5.969e^{-06}$m. This is not smaller than the permissible minimum film thickness of $3e^{-6}m$, 3 micrometers. This minimum film thickness is not too large.

To obtain the optimal lubricating gap profile, the initial gap profile is reduced by the corresponding 87.29% to obtain:

| **Relative Position** | **Film thickness** |
|---|---|
| X(0) = 0.0 | H(0) = 0.127 |
| X(1) = 0.5 | H(1) = 0.133 |
| X(2) = 0.1 | H(2) = 0.153 |

These are the control points for the hundred points defining the optimized geometry of the lubricating film thickness.

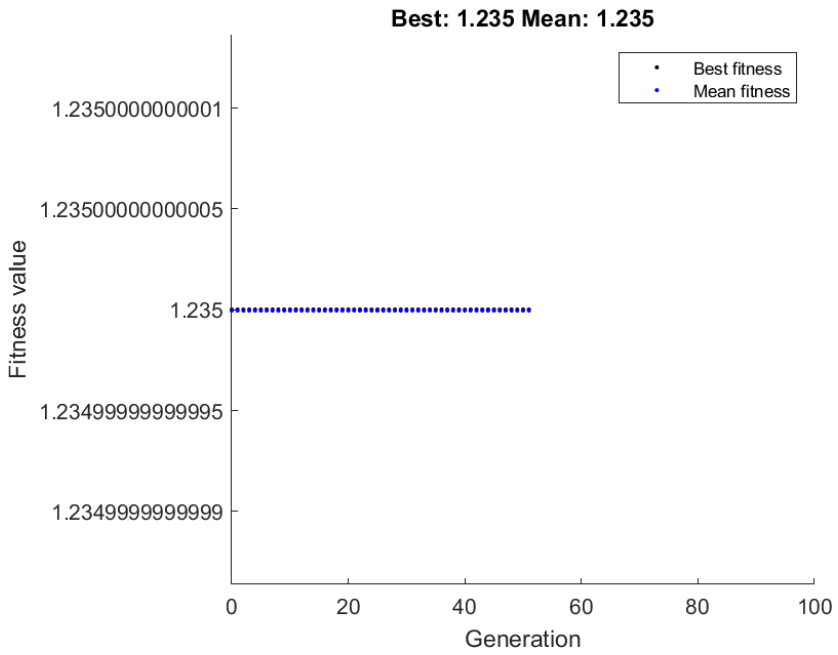


Figure 20: Output graph for GA

Comparing Fig.18 and Fig.21, it is evident that the GA finds a better lubricating gap profile for the general profile considered in Fig.18.

The Genetic Algorithm we see that the find optimal geometries can be found for generally defined lubricating gap geometry.

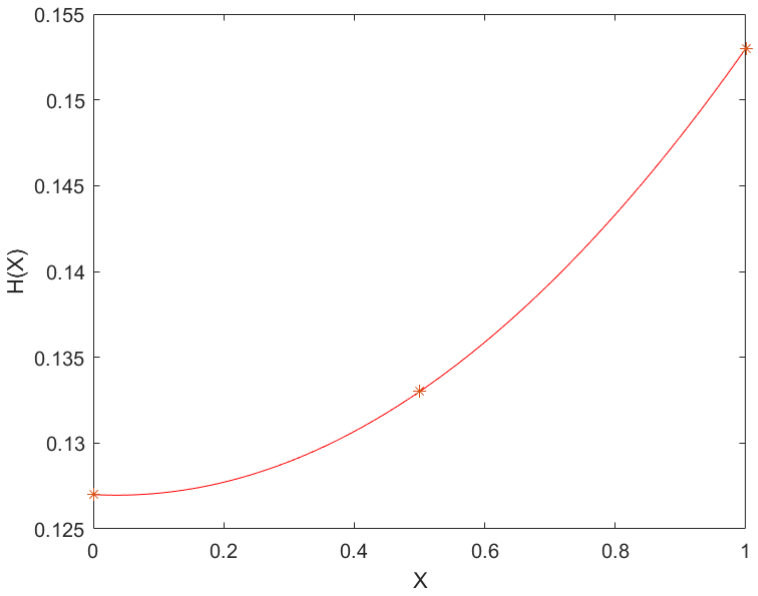


Figure 21: Optimized Lubricating gap profile showing the three control points

# 5 Conclusion

## 5.1 The Optimality Criteria

The choice of the minimum film thickness as the optimality criterion. As mentioned in Section 2.3, the reduction in bearing dimensions for a given minimum film thickness, as is this case, results in reduced power friction losses.

Losses due to friction increase the amount of work the oil pump must do to circulate the lubricant in the internal combustion engine. This increase in the power expended by the oil pump reduces the general efficiency of the system.

Reducing the power friction losses by reducing bearing dimensions for the given minimum thickness, is a good optimality criterion.

## 5.2 Genetic Algorithm: Strengths and Weaknesses

As stated in Section 3.6.1, the Genetic Algorithm has its strengths and weaknesses.

### 5.2.1 Strengths

- It is useful in finding global solution of multi-objective function. The thesis problem is a case in point. The GA was able to find a solution for the multi-objective function of one variable.
- It effortlessly captures multiple non-inferior solutions.
- It uses probabilistic and not deterministic operators. It moves randomly from one solution to another; not following a defined path to finding a solution.
- It is less likely to be trapped in a local minimum. While running the GA for the problem, if the codes were not seeded to return a previously provided solution, the result for each attempt might differ from the next.
- Provides local and global solution.
- In many cases, they are less sensitive to the presence of noise and uncertainty in measurements.

### 5.2.2 Weaknesses

- It requires comparatively less information about the problem. To formulate the objective function, a product of factors was computed. This product of factors was the objective function inputed into the GA. This product was a number. The GA optimized this problem with just one constraint: a constraint on the domain of $x$, that depends on the angles and radii of the thrust bearing. This is too little infor-

mation to describe the working condition of the turbocharger.

- It is computationally time consuming. A single solution of a bearing steady state may include hours of computational time on high-performance computers. This fact makes it practically impossible to use these calculations for multiple repetitive tasks involving the solution of hundreds or thousands of operating states.

- Despite the fact that GA for the thesis problem was relatively simple, coding the equations the equations to generate the required factors for the multiobjective function is time consuming.

## 5.3 Application of Study

The results of this work are not limited to just turbochargers. The idea of using a spline function to describe a general profile for study is not novel, but it holds a lot insight when properly explored. Nature does not make basic or perfect shapes, humans do not either.

The complex shapes must be optimized for better performance: less drag, better aerodynamics, better flight of the golf ball, etc.

The ideas expounded by this work are far reaching into different fields of study.

## 5.4 Questions

It is known that minimizing the friction force reduces the oil film thickness of a hydrodynamic bearing; increasing the oil film thickness increases the load capacity.

It has already been mentioned in the work that optimization problems often require us to impose unrealistic constraints to solve them.

Could weight capacity be increased and friction force be reduced simultaneously?

# 6 References

# References


[1] Avraham, H. (2002). Bearing Design in Machinery: Engineering Tribology and Lubrication. New York: Marcel Dekker.

[2] Talluri, S.K; Hiran, H.(2003) Parameter Optimization of Journal Bearings using Genetic Algorithm. Indian Journal of Tribology. Volume 2 (2003) 1-2, 7-21.

[3] Forsthoffer, M. (2019). Journal (Radial) Bearings. Forsthoffer's Component Condition Monitoring. https://doi.org/10.1016/B978-0-12-809599-7.00004-X.

[4] Haslinger, J., Makinen, R.A.E. (2003). Introduction to Shape Optimization: Theory, Approximation and Computation. Philadelphia: Society for Industrial and Applied Mathematics.

[5] Ozalp, A., Umur, H. (2006). Optimum surface profile design and performance evaluation of inclined slider bearings. Current Science, 90(11), 1480-1491. Retrieved February 20, 2021, from http://www.jstor.org/stable/24091822.

[6] Papalambros P.Y, Wilde, D.J. (2009). Principles of Optimal Design: Modelling and Computation. 2nd edition. Cambridge: Cambridge University Press.

[7] Wasilczuk, M. (2006). Comparison of an optimum-profile hydrodynamic thrust bearing with a typical tilting-pad thrust bearing. Lubrication Science. https://doi.org/10.1002/ls.3010150306

[8] Novotný,P., Jonák, M., Vacula, J. Evolutionary Optimisation of the Thrust Bearing Considering Multiple Operating Conditions in Turbomachinery, International Journal of Mechanical Sciences, Volume 195, 2021, 106240, ISSN 0020-7403, https://doi.org/10.1016/j.ijmecsci.2020.106240.

[9] Novotný, P., Hrabovský, J.,(2020) Efficient computational modelling of low loaded bearings of turbocharger rotors, International Journal of Mechanical Sciences, Volume 174, 2020, 105505, ISSN 0020-7403, https://doi.org/10.1016/j.ijmecsci.2020.105505.

[10] Gropper, D.,, Wang, L., Harvey, T.J., Hydrodynamic lubrication of textured surfaces: A review of modeling techniques and key findings (2016), Tribology International, Volume 94, 2016, Pages 509-529, ISSN 0301-679X, https://doi.org/10.1016/j.triboint.2015.10.009.

[11] Yu, H., Wang, X., Zhou, F. Geometric Shape Effects of Surface Texture on the Generation of Hydrodynamic Pressure Between Conformal Contacting Surfaces. Tribol Lett 37, 123–130 (2010). https://doi.org/10.1007/s11249-009-9497-4.

[12] Bullock, G. N., Denham, M. J., Parmee, I. C., Wade, J. G. (1995). Developments in the use of the genetic algorithm in engineering design. Design Studies, 16(4), 507–524. https://doi.org/10.1016/0142-694x(95)00023-k

[13] Alaa, S., Hamza, T., (2006). A comparison between genetic algorithms and sequential quadratic programming in solving constrained optimization problems. ICGST International Journal on Artificial Intelligence and Machine Learning (AIML). 6. 67-74.

[14] Hashimoto, H. (1998). Optimization of Oil Flow Rate and Oil Film Temperature Rise in High Speed Hydrodynamic Journal Bearings. Tribology and Interface Engineering Series, 34, 205-210.

[15] Xiaopeng, F. (2007). Engineering design using genetic algorithms. Retrospective Theses and Dissertations.15943. https://lib.dr.iastate.edu/rtd/15943.

[16] Rolf Steinbuch,(2010) Successful Application of Evolutionary Algorithms in Engineering Design, Journal of Bionic Engineering, Volume 7, Supplement, 2010, Pages S199-S211, ISSN 1672-6529, https://doi.org/10.1016/S1672-6529(09)60236-5

[17] WAZIRI M.Y., LEONG W.J., HASSAN M.A., and MONSI M. Jacobian Computation-Free Newton Method for Systems of Non-Linear Equations. Journal of numerical Mathematics and stochastic, 2(1):5463, 2010.

[18] STACHOWIAK Gwidon W. and BATCHELOR Andrew W. Engineering Tribology.3. Butterworth-Heinemann, 2005. ISBN 0-7506-7836-4.

[19] LUKE, S. Essentials of Metaheuristics. 2nd ed., 2013. ISBN 9781300549628.

[20] NGUYEN-SCHÄFER, H. Rotordynamics of Automotive Turbochargers. Second Edition. Ludwigsburg, Germany: Springer, 2015. ISBN 978-3-319-17643-7.

[21] Yu, X., Liu, H., Zhu, Z., Wu, Q. Hybrid Genetic Algorithm for Engineering Design Problems.Cluster Comput (2017) 20:263–275 doi 10.1007/s10586-016-0680-8.

[22] Feng, K., Liang-Jun, L., Guo, Z., Zhao, X. (2015). Parametric study on static and dynamic characteristics of bump-type gas foil thrust bearing for oil-free turbomachinery. Proceedings of the Institution of Mechanical Engineers, Part J: Journal of Engineering Tribology. 229.10.1177/1350650115577026.

[23] Zhang, H., Dong, G., Hua, M., Guo, F., Kwai-Sang, C. (2015). Parametric design of surface textures on journal bearing. Industrial Lubrication and Tribology. 67. 359-369. 10.1108/ILT-08-2013-0089.

[24] E. Koç, An investigation into the numerical solution of Reynolds' lubrication equation with special reference to thrust bearings, Tribology International, Volume 23, Issue 6, 1990, Pages 429-437, ISSN 0301-679X, https://doi.org/10.1016/0301-679X(90)90059-X.

[25] Steinbuch, R., Successful Application of Evolutionary Algorithms in Engineering Design, Journal of Bionic Engineering, Volume 7, Supplement, 2010, Pages S199-S211, ISSN 1672-6529, https://doi.org/10.1016/S1672-6529(09)60236-5.

[26] Sawadkosin, P., (2019). Shape Optimization of Machine Components due to Variability of Input Data, Institute of Mathematics, Brno University of Technology.

[27] Charitopoulos AG, Visser R, Eling R, Papadopoulos CI.(2018) Design Optimization of an Automotive Turbocharger Thrust Bearing Using a CFD-Based THD Computational Approach. Lubricants. 2018; 6(1):21. https://doi.org/10.3390/lubricants6010021

[28] Elnemr, Yasser. (2011). Acoustic Modeling and Testing of Exhaust and Intake System Components.

[29] Hydrodynamic Bearings. Retrieved from: https://www.machinedesign.com/mechanical-motion-systems/bearings/article/21812843/hydrodynamic-bearings on 19 May, 2021.

[30] Thomsen, K., Klit, P., Vølund, A., Santos, I. (2012). Modeling of dynamically loaded hydrodynamic bearings at low Sommerfeld numbers. Kgs.Lyngby: DTU Mechanical Engineering. (DCAMM Special Report; No. S144).

[31] Wasilczuk, M. (2015). Friction and Lubrication of Large Tilting-Pad Thrust Bearings. Lubricants, 3(2), 164–180. doi:10.3390/lubricants3020164

[32] Sokolowski, J Zolesio, J.P., (1992), Introduction to Shape Optimization : Shape Sensitivity Analysis, Springer-Verlag Berlin Heidelberg, New York.

[33] Prautzsch, H., Boehm, W., Paluszny, M., (2002) Bezier and B-Splines techniques. Springer-Verlag Berlin Hedeilberg, New York.

# List of Figures